This is Chapter 4 "Some characteristics of shotcrete" from my PhD thesis

Kluckner, A. 2023. Tunnelling at greater depths: Study on the ground and system behaviour when passing a stiff rock block in a weak zone. PhD thesis. Graz University of Technology, Graz, Austria.

The full thesis can be downloaded from the TU Graz repository: LINK

If you have any questions or remarks, you can contact me on

ResearchGate: LINK

or on

LinkedIn: LINK.

Enjoy reading.

Best regards, Alexander Kluckner



# Dipl.-Ing. Alexander Kluckner, BSc

# Tunnelling at greater depths: Study on the ground and system behaviour when passing a stiff rock block in a weak zone

#### DOCTORAL THESIS

to achieve the university degree of Doktor der technischen Wissenschaften

submitted to

Graz University of Technology

#### Reviewers

Em.Univ.-Prof. Dipl.-Ing. Dr.mont. Wulf Schubert Faculty of Civil Engineering Sciences Graz University of Technology, Graz, Austria

Univ.-Prof. Dr. Nobuharu Isago Faculty of Urban Environmental Sciences Tokyo Metropolitan University, Tokyo, Japan

# Contents

Li	st of	Figures	xxi
Li	st of	Tables	xxix
Li	st of	Acronyms, Symbols, and Notations	xxxv
1	Intr	roduction	1
	1.1	Research motivation	. 1
	1.2	Research questions	. 4
	1.3	Methodology	. 5
	1.4	Thesis structure and objectives	. 6
	1.5	Research limitations	. 7
2	Abo	out fault zones and block-in-matrix rocks	9
	2.1	Brittle fault zones	. 12
	2.2	Block-in-matrix rocks	. 14
3	Son	ne properties of rocks and rock masses	19
	3.1	Geometric properties of bimrock blocks	. 19
		3.1.1 Block shape	. 19
		3.1.2 Block location and orientation	. 21
		3.1.3 Block size	. 21
	3.2	Mechanical properties of rocks and rock masses	. 22
		3.2.1 Shear strength of the matrix material	. 22
		3.2.2 Uniaxial compressive strength of the matrix material	. 28
		3.2.3 Shear strength of the block material	. 28
		3.2.4 Uniaxial compressive strength of the block material $\ \ldots \ \ldots \ \ldots$	. 28
		3.2.5 Tensile strength	. 30
		3.2.6 Dilation angle	. 32
		3.2.7 Poisson's ratio	. 33
		3.2.8 Density	. 36
		3.2.9 Young's modulus	. 36
		3.2.10 Block-matrix contacts	. 40
4	Son	ne characteristics of shotcrete	45
	4.1	Hardening of concrete	. 47
	4.2	Origin of strength and stiffness growth	. 47
	4.3	A note on the behaviour under pressure	. 48
	4.4	About strain in shotcreted tunnel linings	. 49
	15	Postroints	50

CONTENTS

	4.6	Strain	n components	51
		4.6.1	Elastic (instantaneous) strain	52
		4.6.2	Thermal elastic (instantaneous) strain	52
		4.6.3	Shrinkage (delayed) strain	54
		4.6.4	Creep (delayed) strain	57
		4.6.5	Plastic (instantaneous) strain	60
		4.6.6	Irrecoverable strain due to ageing	62
	4.7	Peak	strain	62
	4.8	Shotc	rete strength	63
	4.9	Shotc	rete deformability	66
		4.9.1	Poisson's ratio	67
		4.9.2	Empirical approximation	67
5	The	ermo-cl	nemo-mechanical shotcrete model	69
	5.1	Displa	acement and strain field	70
	5.2	Shotc	rete model	71
		5.2.1	Chemo-thermal coupling	73
		5.2.2	Thermo-mechanical coupling $\ldots \ldots \ldots \ldots \ldots \ldots$	74
		5.2.3	Chemo-mechanical coupling	74
6	Stif	f block	next to excavation (2D): Parametric study	81
	6.1	Nume	erical model setup	82
		6.1.1	Modelling of system features	82
		6.1.2	Modelling of material behaviour	84
		6.1.3	$\operatorname{Mesh} \ldots \ldots$	86
		6.1.4	$\label{eq:Model size of Model size} Model size$	87
		6.1.5	Boundary conditions and initial state	87
		6.1.6	Solve criterion and damping	87
		6.1.7	Excavation method	88
	6.2	Nume	erical input parameters	89
		6.2.1	Tunnel shape and size $\hdots$	90
		6.2.2	Primary stress state	90
		6.2.3	Block shape	90
		6.2.4	Block location and orientation $\dots$	90
		6.2.5	Distance of the block from the tunnel and block size $\ \ldots \ \ldots \ \ldots$	94
		6.2.6	Internal angle of friction of the matrix material	94
		6.2.7	Internal angle of friction of the block material	94
		6.2.8	Cohesion of the matrix material	95
		6.2.9	Uniaxial compressive strength of the matrix material	96
		6.2.10	Uniaxial compressive strength of the block material	97
		6.2.11	Cohesion of the block material	98
		6.2.12	Tensile strength	98
		6.2.13	Dilation angle	100
		6.2.14	Poisson's ratio	100
		6.2.15	Density	100
		6.2.16	Young's modulus	100
		6 2 17	Interface properties	101

CONTENTS xv

	6.3	Evalu	ation approach	103
		6.3.1	Angular deviation of in-plane tunnel displacement vectors	105
		6.3.2	Total in-plane tunnel displacements	107
		6.3.3	Shear strain increment along tunnel periphery	108
		6.3.4	Maximum in-plane block-matrix interface slip, and other interface related	
			variables	109
		6.3.5	Block bending	109
		6.3.6	Horizontal evaluation plane	
		6.3.7	Path of highest secondary in-plane major principal stresses	
		6.3.8	Parameter development with ongoing relaxation	
		6.3.9	Zone-by-zone comparison of different cases	
			Orientation of stresses along block periphery	
			Spalling limit and damage threshold	
			Work	
	6.4		ts: Summary	
	0.1	6.4.1	In-plane block-matrix interface slip	
		6.4.2	Shear strain increment	
		6.4.3	Block deformation	
		6.4.4	Block displacement	
		6.4.5	Path of the highest secondary in-plane major principal stresses	
		6.4.6	Shear strain increment along tunnel periphery	
		6.4.7	Displacement of the tunnel periphery	
		6.4.8	Yielded zones	
		6.4.9	Block failure	
			In-plane stresses	
			Orientation of in-plane stresses	
			Elastic work	
	6.5		pretation and discussion	
	0.0	6.5.1	The block-matrix interface rules	
		0.0.1		
		6.5.2	•	
		6.5.3	Small block distance: hazardous	
		6.5.4	Identification on site? It depends	
		6.5.5	Underestimation of the situation	
		6.5.6	About installing support	157
		6.5.7	On dynamic effects	
		6.5.8	Most probable scenario	158
7	Stiff	f block	next to excavation (3D): Supplementary study	159
	7.1		erical model setup	159
		7.1.1	Modelling of system features	159
		7.1.2	Mesh	160
		7.1.3	Model size	160
		7.1.4	Boundary conditions and initial state	
		7.1.5	Construction sequence and excavation method	
	7.2		erical input parameters	161
		7.2.1	Block shape	161
		7.2.2	Block location	
		_		

CONTENTS xvi

		7.2.3 Block distance from the tunnel	61
	7.3	Evaluation approach	61
	7.4	Results	62
	7.5	Interpretation and discussion	67
8	Fibi	re optic monitoring section: Data evaluation 1	69
	8.1	Distributed fibre optic sensing	
	8.2	Geological and hydrogeological conditions	
	8.3	Rock mass types	
	8.4	Primary stress state	
	0.1	8.4.1 General	
		8.4.2 Primary stress at the analysed section	
	8.5	Tunnelling method	
	0.0	8.5.1 Excavation sequence	
		8.5.2 Support	
		8.5.3 Work steps	
	0.6	•	
	8.6	Position of monitoring devices	
	8.7	Observed system behaviour: Geodetic measurements	
		8.7.1 Time-dependent displacements	
		8.7.2 Out-of-plane displacements	
		8.7.3 In-plane displacements	
	8.8	Observed system behaviour: DFOS	
		8.8.1 Strain in the circumferential and longitudinal direction	
		8.8.2 Evolution of strain with time	
		8.8.3 Strain rate	
	8.9	Observed system behaviour: Temperature	96
9	Fib	re optic monitoring section: Calibration case (3D)	01
	9.1	Limitations	02
		9.1.1 Time-dependent rock deformation	02
		9.1.2 Swelling	02
		9.1.3 Porewater pressure	02
	9.2	DFOS section: Strain components utilising a micromechanical model 2	03
		9.2.1 Neglecting thermal strain	04
		9.2.2 Neglecting shrinkage strain	05
	9.3	Burgers model	05
		9.3.1 Basic rheological models	07
		9.3.2 Combined rheological models	07
	9.4	•	10
		9.4.1 Modelling of system features	12
		9.4.2 Modelling of material behaviour	
		~	14
			15
			15
			15
		r o	16
		9.4.8 Creep time step	
		one creep time step	-

CONTENTS xvii

	9.5	Numerical input parameters	20
		9.5.1 Tunnel shape and size $\dots \dots \dots$	20
		9.5.2 Primary stress state	20
		9.5.3 Rock mass	20
		9.5.4 Backfill	25
		9.5.5 Shotcrete lining	25
		9.5.6 Rock bolts	33
	9.6	Evaluation approach	36
	9.7	Results	36
	9.8	Interpretation and discussion	40
10		,	43
	10.1	Limitations	
	10.2	Geological and hydrogeological conditions	
	10.3	Rock mass types	
	10.4	Primary stress state	
		10.4.1 General	
		10.4.2 Primary stress at the analysed section	
	10.5	Tunnelling method	
	10.6	Position of monitoring devices	
	10.7	Observed system behaviour: Geodetic measurements	
	10.8	Numerical model setup	
		10.8.1 Modelling of system features	
		10.8.2 Modelling of material behaviour	
		10.8.3 Mesh	
		10.8.4 Model size	
		10.8.5 Boundary conditions and initial state	
		10.8.6 Construction sequence	
	10.9	Numerical input parameters	
		10.9.1 Tunnel shape and size	
		v	60
			61
		9	67
			68
		**	68
			69
	10.12	Interpretation and discussion	71
11	Disc	ussion 2'	77
	11.1		77
	11.2	·	78
	11.3		79
	11.4		79
	11.5		81
	11.6		81
			81
		11.6.2 Tunnel support	
		**	

CONTENTS xviii

	11.6.3 Tunnelling sequence	284	
12 Con	aclusion	<b>285</b>	
Bibliog	graphy	287	
Appen	Appendix A: Equations 3		
A.1	Stress invariants	317	
A.2	Strain invariants	317	
A.3	Mohr-Coulomb failure criterion	318	
A.4	Size of the yield zone in a homogeneous, isotropic rock mass	318	
A.5	Elastic secondary tangential in-plane stresses around a circular opening in a		
	homogenous, isotropic medium	319	
A.6	Elastic secondary tangential in-plane stresses around an elliptic opening in a		
	homogenous, isotropic medium	320	
Appen	dix B: Some mechanical properties of rocks	321	
В.1	Tensile strength	321	
2.1	B.1.1 Johnston (1985)		
	B.1.2 Kluckner (2012)		
	B.1.3 Rostami et al. (2016)		
B.2	Dilation angle		
5.2	B.2.1 Terminology		
	B.2.2 Kluckner (2012)		
B.3	Poisson's ratio		
B.4	Young's modulus		
2.1	20446 2 4004444	0_0	
Appen	dix C: Stiff block next to excavation (2D): Parametric study	329	
C.1	Numerical model setup		
	C.1.1 Evaluation of constitutive model for matrix material		
	C.1.2 Evaluation of minimum in-plane model size		
	C.1.3 Evaluation of solve limit	337	
	C.1.4 Evaluation of excavation method	342	
C.2	Numerical input parameters	343	
	C.2.1 Mechanical properties of model features	343	
	C.2.2 Evaluation of interface stiffnesses	350	
C.3	Results: Details	355	
	C.3.1 In-plane block-matrix interface slip	355	
	C.3.2 Shear strain increment	370	
	C.3.3 Block deformation: Bending	385	
	C.3.4 Block deformation: Change in the block height	391	
	C.3.5 Block deformation: Change in the block width	393	
	C.3.6 Block displacement	396	
	C.3.7 Path of the largest secondary in-plane major principal stresses $\dots \dots$	400	
	C.3.8 Shear strain increment along tunnel periphery	405	
	C.3.9 Displacement of the tunnel periphery	411	
	C.3.10 Yielded zones	425	
	C.3.11 Block failure	438	

CONTENTS			
C.3.12 In-plane stresses	457		
C.3.13 Orientation of in-plane stresses	472		

C.3.14 Elastic work	485
Appendix D: Fibre optic monitoring section: Data evaluation	497

# Chapter 4

# Some characteristics of shotcrete

Concrete (or shotcrete = sprayed concrete) is a cement-based construction material. Its constituents (i.e., cement, aggregates, water, admixtures, and additions) control the properties of the hardening and hardened concrete and are mixed in a way that the requirements are met ([68, p. 395]). The fundamental difference between conventional pre-cast concrete and shotcrete is the moment of initial loading ([129, p. B-5]; exception: loading due to self-weight). In tunnelling, shotcrete usually is loaded externally the moment it is applied to the rock mass.

Sections following summarise some specifics of concrete and shotcrete important when dealing with such material in conventional tunnelling. The improvement of shotcrete—by using, e.g., new cements, additives, and mixing ratios—is a hot topic in research and industry (cf. [208, p. 380]). The need to reduce CO<sub>2</sub> emissions triggers some development. Thus, approaches and related settings used in the past to model shotcrete mathematically may not be suitable anymore for today's shotcrete boosted with chemicals. The information presented below is not complete. It rather shows basic concepts. To model the shotcrete behaviour accurately, there is no way around to perform tests on the material to be used. Also, the boundary conditions (e.g., lining thickness, ambient temperature) are not to be ignored. Using settings of other shotcrete mixes and other projects, it is difficult (or impossible) to estimate the difference in the modelled behaviour and relating consequences.

Besides the fact that design standards for reinforced concrete do not apply directly to shotcrete, in particular if the shotcrete is young (cf. [208, p. 369f], [209] in [388, p. 140]), the same recommendations need to be taken seriously: if curing conditions at the site (significantly) deviate from those at standard tests, or from those the design standards and guidelines apply to, investigations and tests need to consider them (cf., e.g., [68, p. 416] referring to the strength development of concrete, and [10, p. C-41] referring to creep tests). Then, and also when comparing or analysing published test date (is the comparability given?), several aspects decide upon the results: e.g., sealed or unsealed conditions, humidity, temperature, sample size and shape, and loading rate (mechanical or thermal load). The aspects are similar to when rock is tested (cf. [199, p. 14ff]). For example, sustained too low or too high temperatures during the curing of concrete can affect its strength and stiffness development negatively ([42, p. 37], [69, 70] in [388, p. 21, 144]). But not only the environmental conditions are decisive. The characteristics and share of each concrete's constituent are too. For example, the relations between the water-cement ratio and the compressive strength are not unique, depend in particular

<sup>&</sup>lt;sup>1</sup>Shotcrete is not a special concrete. It is still concrete but with particular characteristics and installed differently than cast-in-place concrete. Concrete technological principles are the same for both concrete and shotcrete. However, they need to be adapted. (cf. [129, p. B-31f], [208, p. 305])

<sup>&</sup>lt;sup>2</sup>[289, p. 6, 26] uses the term *young* to refer to shotcrete at an age of up to 24 hours.

on the type of cement and aggregates, and require specific tests on samples using mixes intended for the construction site ([68, p. 401]; cf. also [388, p. 142] referring to the calibration of creep models). Now, if the settings of tests and conditions in the laboratory or at the construction site are outside the scope of design standards and guidelines, equations and other suggestions cited therein are probably not applicable anymore. The same applies to model fittings. They usually relate to one particular concrete or setting only.

In analytical or numerical calculations, empirical approximations account, for example, for the development of individual strain components and strengths. Either the formulations are approximations, or the input parameters, or both. Some of the following sections briefly describe which formulations five well-known models utilise to simulate the behaviour of shotcrete. That are:<sup>3,4</sup>

- Schubert (1988) [358]: He uses the analytical rate of flow method by [107]. It's a one-dimensional consideration;
- Schädlich and Schweiger (2014) [348]: They formulate a three-dimensional constitutive model within the framework of elastoplastic strain hardening/softening plasticity. [349] report on the application of the model;
- Schütz et al. (2011) [368]: They, too, formulate a three-dimensional constitutive model within the framework of elastoplastic strain hardening/softening plasticity. For more details on the model, refer to [369];
- Meschke (1996) [260]: He constitutes a three-dimensional multisurface model based on viscoplasticity considering also hardening and softening mechanisms. Note that the follow-up paper by Meschke et al. (1996; [261]) comprises the calibration of the model;
- Neuner et al. (2017) [276]: Their three-dimensional model bases on the damage plasticity model for concrete proposed by [134]. They've modified it to allow for the simulation of shotcrete behaviour. It also accounts for hardening and softening mechanisms. For corrections, correlations, and applications, refer to [275, 277, 278].

Note that [276, 348, 368] use old data for validation (referring to the year of the publication describing the individual model);<sup>5</sup> namely from [10, 71, 129, 173, 265, 271, 371, 387]. Probably science lacks of published validation data. Anyway, it must be assumed that the latest shotcrete types differ in the behaviour. A general validity of the fittings is not guaranteed (cf., e.g., [388, p. 131] referring to fittings of creep data, [208, p. 352] referring to the transfer of results from one construction site to another, [10, p. D-9] and [42, p. 34] both referring to the temporal development of strength). Making it more difficult and stated already above, even if the shotcrete to be installed at the construction site is tested, conditions in the laboratory can differ (significantly) from those at the site in magnitude and duration (cf. [352, p. 22] referring to the temporal development of strength).

Recent PhD theses dealing with shotcrete are, for example, [57, 169].

<sup>&</sup>lt;sup>3</sup>This list does not intend to be exhaustive regarding concrete or shotcrete models. The list and descriptions in the following sections shall only summarise how other selected researchers have proceeded in the past.

<sup>&</sup>lt;sup>4</sup>Note that only in this chapter some references from the following list are cited in a different style (author-year citation) to ease the differentiation for the reader.

<sup>&</sup>lt;sup>5</sup>In a follow-up paper, Neuner et al. (2017; [275]) present results from recently performed tests on shotcrete samples from the Brenner Base Tunnel project. This paper validates the model introduced in [276] anew.

## 4.1 Hardening of concrete

The hardening concrete comprises aggregates, unhydrated cement and hydrates (summarised as the solid skeleton), and fluid-saturated pores ([155, p. 692])<sup>6</sup>. Hydrates are the products of the physical and/or chemical combination of free water and unhydrated cement. The water is then combined in the solid phase (= hardened cement gel) and is nonevaporable. The term *ageing* relates to this process ([260, p. 3123]). [401, p. 785ff]

The moment the constituents are mixed, a chemical imbalance between water, cement, and hydrates (as soon as some have formed) exists. This difference in chemical potential (also termed affinity) causes the chemical reaction to initiate and to proceed ([155, p. 693f]) until a balanced state is reached. This process is termed cement hydration<sup>7</sup>. The initial imbalance depends on the initial temperature and the design of the mixture (e.g., cement type, water-cement ratio) ([401, p. 790], [68, p. 62]), and a minimum amount is required to activate the hydraulic reactions in the first place (i.e., minimum activation energy required; [300, p. 912]). Here, the hydration heat amplifies the activation (thermal activation; cf. [401, p. 787])

Hydrates starts to grow at the contact surface between the unhydrated cement and the free water (not chemically bounded yet). With some hydrates having formed, it takes longer for the remaining free water to diffuse (because of thermodynamic imbalance between free water and water bound in hydrates) to the remaining unhydrated cement through the hydrates already formed ([401, p. 787f]; cf. Fig. 5.2 on p. 71). Therefore, the mass of hydrates already formed determines the evolution (i.e., rate) of hydration ([158, p. 2104]). The hydration degree is the ratio of current to final hydration extent and is linearly proportional to the mass (or volume) of hydrates formed ([7] in [302, p. 230], [208, p. 368], [314] in [401, p. 790]). It varies between 0 and 1.

# 4.2 Origin of strength and stiffness growth

Primarily, strength (e.g., compressive and tensile strength) increases because the share of solids in mass per unit volume increases with ongoing hydration. The increase in strength is proportional—at early-age concrete quasi-linear ([263] in [155, p. 693])—to the amount of formed solid hydration products ([370, p. 286]). The increase in the amount of strong, stiff solids, the decrease in the amount of weak, soft fluid-saturated spaces, and the creation of bonds between adjacent solids is also the origin of the increase in stiffness (cf. [370, p. 284]).

However, growth in strength and stiffness, both of which are usually desired, is accompanied by an undesired reduction of the elastic strain limit (i.e., damage threshold; [402, p. 1123]) and ductility<sup>8</sup> ([348, p. 103]). This is because spaces allowing for movement of fluids in case the shotcrete is loaded continuously are replaced by stiff brittle solids.

Secondarily, the consumption of free water during cement hydration causes the capillary pressure between the liquid and the gaseous phase saturating the pores to increase, which also stiffens the compound ([401, p. 788]).

The phenomenon described here is termed *chemical hardening* ([402, p. 1125f]). It is not to be confused with *work* or *strain hardening* related to elastoplasticity<sup>9</sup>.

 $<sup>^6\</sup>mathrm{It}$  is assumed that the authors refer to an unadjusted concrete. Usually the concrete comprises additives and admixtures to optimise its behaviour to the project specific needs.

<sup>&</sup>lt;sup>7</sup>Hydration: Attachment of water molecules to solute particles. [16, p. 191]

<sup>&</sup>lt;sup>8</sup>Ductility describes the material's capability for (large) deformation upon loading without failure. (cf. [149, p. 35], [337, p. 3], [419, p. 148])

<sup>&</sup>lt;sup>9</sup>Hardening: Stress continues to increase with strain beyond the yield limit of the material. [181, p. 86]

## 4.3 A note on the behaviour under pressure

All materials exhibit a distinctive behaviour when subjected to a specific mechanical loading (e.g., water pressure acting on a dam) or when exposed to a specific environment (e.g., extension or shortening in case of temperature change). The design of structures requires a correlation between the *action* and *reaction*. Such a correlation is called *constitutive equation*. Fig. 4.1 exemplifies the reaction (i.e., individual strain components) of a hardening concrete specimen exposed to *normal* constant environmental conditions (i.e., constant humidity and temperature) and subjected to a sustained constant compressive load (= action).

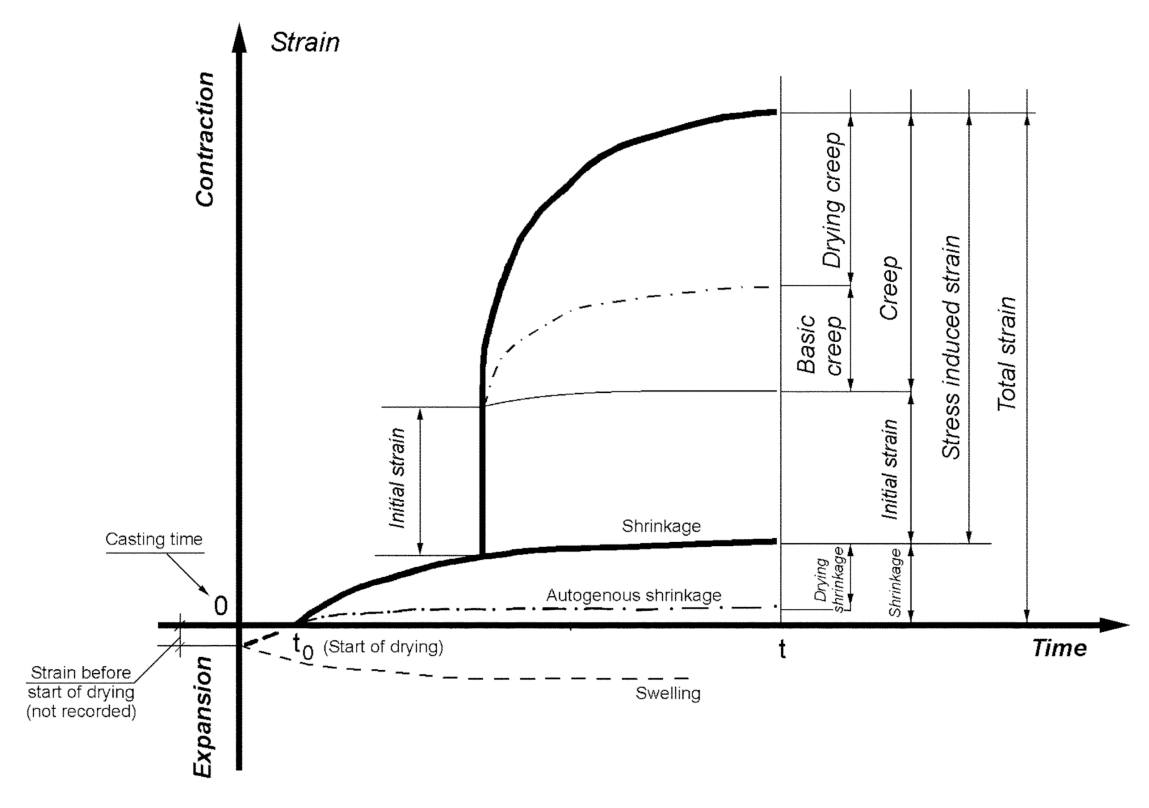


Figure 4.1: Development of strain components of a concrete specimen subjected to a sustained constant compressive load (uniaxial compression test; the moment of load application equals the moment *initial strain* develops) under constant environmental conditions (from [4, Fig. 1.1, p. 2]).

The development of the strain components shown in Fig. 4.1 all depend on the material properties, some of them depend on the environmental conditions, some of them are time-dependent, and others depend on the loading level (mechanical loading or temperature change) only. Some dependencies are described in the following sections. Note that the illustrated development is valid only for a hardening concrete specimen in an uncracked state at the macrolevel (i.e., scale of laboratory test specimen), meaning that the applied load is below approx. 30–40% of the compressive strength (i.e., below the limit of proportionality; cf. Section 4.9 on p. 66) at the moment of load application. Above this threshold, microcracks grow ([118] in [388, p. 16])—resulting in *strain hardening*—, link with each other, and, eventually, form macrocracks. Also, the specimen must not be exposed to any aggressive media (e.g., chemicals), which would alter the specimen's integrity and affect the hardening process. The development of the material properties and, therefore, of the individual strain components might be also different for concrete specimens placed underwater.

<sup>&</sup>lt;sup>10</sup>Note that the reference the graph is taken from refers to hardened concrete. Anyway, the graph shows the onset of autogenous shrinkage which is because of hydration reactions when the concrete sets (cf. [4, p. 3]).

## 4.4 About strain in shotcreted tunnel linings

Engineers make use of circular linings in tunnels and other curved underground openings because of their high load-bearing capacity as soon as a stress ring (or stress arch if the lining is not closed) forms in the circumferential direction ([260, p. 3158]). The shotcrete lining usually features approximately a biaxial compressive stress state ([260, p. 3158], [129, p. B-5, E-24]). However, often not the compression is problematic but tensile stresses (even if occurring only locally or for a short period). And then tensile strength dominates the lining behaviour ([347, p. 7]).

In the DFOS section (cf. Chapter 8 on p. 169), tensile strain occurred on the first days after the shotcrete application, mostly at the ends of the top-heading lining before the ring was closed. The displacement pattern suggests that the unfavourable orientation of the foliation planes predominantly causes this elongation. At early ages, however, cracking of the lining is mainly because of restrained thermal and chemical shrinkage ([402, p. 1123]). Similarly, [210] (cited in [277, p. 2]) report about cracking because of unfavourable bending moments originating from the deformation of the heterogeneous ground and because of tensile loading induced by shrinkage and thermal gradients.

Because of hydration, temperature rises within the shotcrete (cf. Section 8.9 on p. 196). During this time, when the shotcrete is young, the elastic modulus is low and the creep rates are high. Thus, thermal expansion does not result in significant compressive stresses. However, as soon as the hydration process abates, the shotcrete cools off and shrinks (i.e., thermal shrinkage) ([401, p. 785]). The shotcrete is then older, being less ductile. The bond between the lining and the rock mass, but also between individual shotcrete layers, restrains the deformation to some extent. Autogenous shrinkage, which also takes place from the beginning on, further worsens the situation. Now, if the compressive loading is too low, which often is the case only at the beginning, tensile stresses might get induced locally and, if exceeding the tensile strength, the lining may crack (cf. [388, p. 126]). Thus, the influence of shrinkage and, in particular, of autogenous shrinkage—because it starts already before the shotcrete sets—must not be underestimated. According to [155, p. 696], it can be twice or three times the cracking strain of concrete ( $\approx 0.01\%$ ). Hence, the early age deformability in tension is of crucial importance ([368, p. 840]). [388, p. 43]

One must not forget that in-plane strain and stresses affect out-of-plane strain and stresses, and vice versa (cf., e.g., [129, p. B-72] referring to creep strain). The moment the shotcrete has been applied to the rock mass, several phenomena causing strain compete with each other ([401, p. 785]). Along its circumference, the lining is heterogeneous in terms of thickness, application quality, restraints, and environmental conditions and, thus, must deform non-uniformly. Because of anisotropies and imperfections, a strongly heterogeneous state of stress and deformation results in the lining ([129, p. B-36]). According to [388, p. 43], it is the non-uniform nature of volume change which causes cracking rather than the magnitude of shrinkage.

For conventional tunnel drives excavated in sequences (e.g., top and bench/invert heading), like it is for the calibration case (cf. Chapter 9 on p. 201) and for the evaluation case (cf. Chapter 10 on p. 243), tensile stresses might be introduced in the lining when the follow-up heading (e.g., bench/invert heading) undercuts the preceding heading (e.g., top heading) (cf. [129, p. B-65]). [388, p. 117f] kind of disagrees as he states: "Unloading is probably of limited relevance to the lining of a single tunnel constructed on its own with a top heading, bench and invert excavation sequence, since little unloading would be expected to occur." At the DFOS

 $<sup>^{11}</sup>$ According to [121, p. 87], the decrease in tensile strength because of shrinkage cracks is more pronounced for high strength concrete than for normal strength concrete.

section, which is used as the calibration case, a decrease in the compressive strain but also a switch from compressive to tensile strain can be observed when the bench/invert heading passes the section approx. five days after the top-heading excavation (cf., e.g., Fig. 8.13 on p. 192). However, the magnitude of tensile strain is low. The maximum tensile strain occurs within the first 38 hours after the reference measurement (cf. Section 8.8.2 on p. 190). Whether a particular amount of tensile strain at a particular moment is problematic is not to be judged based on the amount only. It rather depends on the change in deformability and strength coming along with ageing of the concrete material. Strength and stiffness increase, but ductility and creep effects decrease ([348, p. 103, 106]). With time, a transition from a ductile to a brittle material response takes place ([337, p. 1, 3], [368, p. 842]) and the strain at peak strength, both for compression and for tension, decreases ([368, p. 836]).

At last, it must be highlighted that in deep tunnels with large deformations the lining rarely fails because of bending and related tensile fractures but because of shearing ([129, p. B-14]). In case of bending and local tensile failure, the lining still makes up a stable multi-hinged arch or ring capable of bearing considerable load ([129, p. B-14]). In general, changes in the lining's stress and strain state are mainly deviatoric rather than hydrostatic ([388, p. 118]). The probability of shear failure may increase in case the rock mass comprises a few highly effective discontinuities crossing the tunnel.

#### 4.5 Restraints

The reaction of the system (here the shotcrete lining) upon loading (mechanical and/or thermal) depends on the system's boundary conditions (here in terms of mechanical constraints) which, in addition, affect the evolution of the system's strain components ([353, p. 23]).

Fig. 4.2 illustrates the consequences of different degrees of restraint. A temperature load acts on a fixed concrete beam that hardens. The temperature increases because of the hydration heat during the hardening process. The beam expands. Because horizontal deformation is prevented on both ends of the beam, stresses get negative (i.e., compressive stresses). Once the hydration has reached its peak, the structure cools off. As the temperature decreases, the beam contracts and introduces tensile stress increments. Note that up to that moment the concrete has hardened already to some degree and features a higher strength and stiffness than in the initial state. Now think on the stiff aggregates in the concrete. They also restrain deformation. If the difference in the deformation of a particular aggregate and of the hardened cement or cement paste surrounding this aggregate is too large (i.e., the degree of restraint is too high), and if the total tensile stress exceeds the current tensile strength of the cement, there the concrete cracks.

At the concrete specimen of which the resulting strains are illustrated in Fig. 4.1, constraints resulted due to the frictional resistance at the contact of the specimen ends with the pressure plates.

At shotcrete tunnel linings, restraints mainly arise because of the bond between the lining and the rock mass to which the shotcrete is applied, the bond between the new lining segment (e.g., at the current excavation round) and the old lining segment (e.g., at the previous excavation round), and if the lining abuts, for example, on the unsupported temporary top-heading invert. Fig. 4.3 schematically illustrates the in-plane situation of a top heading. If the top-heading feet and the unsupported top-heading invert are apart from each other, and if there is, theoretically, no bond between the lining and the surrounding rock mass, the feet can displace downwards freely (cf. Fig. 4.3a). Anyway, this scenario is unrealistic. Rather because of the bond and the

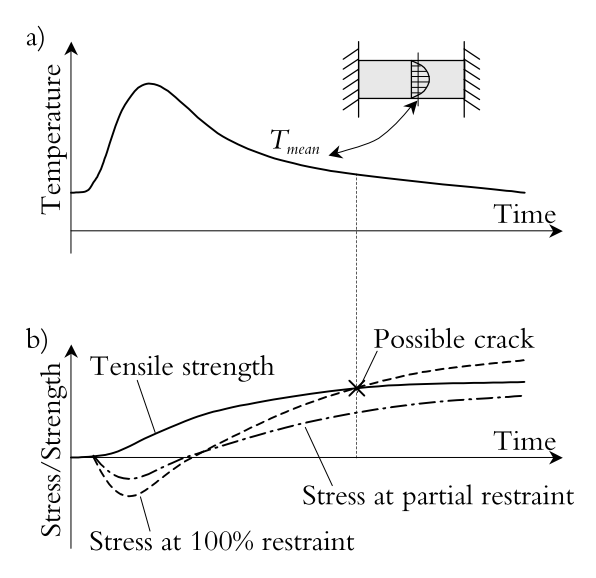


Figure 4.2: Schematic illustration of the restraint problem using the example of a fixed hardening concrete beam subjected to temperature load (from [282, Fig.1, p. 3]): (a) development of the mean temperature with time, (b) development of the stress and the strength with time.

fact that at any one moment the feet touch and get pushed into the rock mass (cf. Fig. 4.3b), deformation is restrained and stresses increase in the lining. Note that whether locally the rock mass displaces downwards relative to the lining or the lining relative to the rock mass depends, for example, on the loading of the system and the stiffness contrast between the lining and rock mass material. Restraints also arise when a lining features two or more layers applied at different times. Then, the shotcrete material of the individual layer differs in strength and stiffness. Other sources for restraints for the shotcrete to deform are, for example, wire meshes, lattice girders, and bolts but also the stiff aggregates in the shotcrete composite.

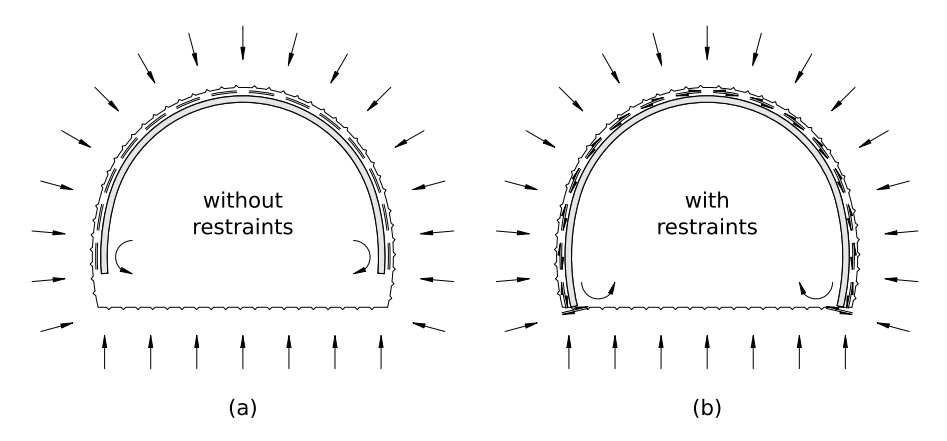


Figure 4.3: Schematic illustration of two in-plane scenarios of a top heading different in the degree of restraints: (a) without restraints (theoretical; unrealistic), (b) with restraints (realistic).

# 4.6 Strain components

Fig. 4.1 (p. 48) lists most important strain components of a concrete specimen under compressive loading. It misses the plastic strain as the load applied is below the yield strength. The following subsections briefly describe each of the strain components.

#### 4.6.1 Elastic (instantaneous) strain

The moment an external mechanical load is applied to (or is removed from) the shotcrete, it reacts instantaneously and deforms according to its materials' elastic properties. Elastic strain develops. The amount of elastic strain depends on the load increment (or decrement) and on the stiffness properties of the shotcrete at the moment of load application (or removal). The shotcrete is a compound of solids and fluid-saturated pores each featuring a different stiffness. As the concentration of solids and fluid-saturated pores changes as cement hydration proceeds, the overall stiffness of the compound<sup>12</sup> changes as well (cf. Section 4.2 on p. 47). This is often termed ageing ([26] in [401, p. 785]; cf. also Section 4.1 on p. 47).

For an uniaxial mechanical load, the elastic strain component results to

$$\Delta \varepsilon_{el,\sigma}(t) = \frac{\Delta \sigma}{E(t)}; \tag{4.1}$$

with

 $\Delta \varepsilon_{el,\sigma}(t)$  elastic strain increment (or decrement) due to uniaxial mechanical load [m/m],

 $\Delta \sigma$  stress increment (or decrement) (compression or tension) [N/mm<sup>2</sup>],

E(t) Young's modulus of the concrete at the moment of loading  $[N/mm^2]$ .

The strain increment (or decrement) depends on the age of the concrete—indicated by the term (t)—as the concrete's Young's modulus changes with the curing level.

#### 4.6.2 Thermal elastic (instantaneous) strain

Thermal strain stems from the fact that the motion of the materials' atoms depends on the temperature ([16, p. 267]). At higher temperatures the motion is larger. And because of the repelling forces between atoms, the atoms then need more space and the volume increases. The thermal motion is smaller and atoms need less space if the temperature decreases. Then the volume decreases as well. Thermal strain is elastic as long as the repelling forces do not outweigh the attracting forces. It is similar for elastic strain upon mechanical loading. Note that with increasing pressure (applied externally) the distance between atoms decreases and the repulsion, motion, and temperature increase ([16, p. F6]). [119, p. 1-5, 14-9]

This concept above suggests that lateral elastic deformation upon axial loading (approximated with the Poisson's ratio) results because the motion of atoms aligns with the principal loading axes in a way so that the difference in repulsive and attractive forces gets a minimum (cf. [119, p. 2-5, 12-10], [198, p. 187]).

The concept also suggests that the behaviour of a material strongly depends on the matter's atomic structure. Thus, any empirical concept (e.g., Young's modulus) cannot be more than—and is by definition—an approximation.

Coming back to the shotcrete lining, because of the exothermic character of the hydration process, temperatures in the concrete can increase significantly within a few hours ([401, p. 790]). In massive structures, they can be up to 50 °C ([401, p. 785]). When the rate of hydration slows down, the temperature decreases again ([401, p. 785]) and balances with the temperature of the surrounding environment after some time. The variation in temperature causes the shotcrete to enlarge in case of temperature increase and to shorten in case of temperature decrease.

 $<sup>^{12}</sup>$ In isotropic elasticity, the stiffness is described with the Young's modulus, E, and the Poisson's ratio,  $\nu$ , (cf. Section 4.9 on p. 66), or with the bulk modulus, K, and the shear modulus, G.

The development of concrete temperature with time depends on the hydration process, the rate of external heat supply provided by conduction and volumetric heat sources ([402, p. 1125]), and the thermal capacity and conductivity ([353, p. 9]). Any of these contributors is very material, element, and project specific. For example, if the initial temperature at the moment of shotcrete application is lower, the later the concrete sets and the longer the hydration process lasts (cf. [42, p. 36f]). The external heat supply depends on the rock mass conditions (e.g., rock type, groundwater flow), the activity of heavy machines nearby, and the air supply system. And the thermal characteristics of the lining itself are determined by the linings' dimensions, the used type of aggregates, and the moisture state ([68, p. 62]).

According to [215] (cited in [388, p. 41]), the coefficient of thermal expansion,  $\alpha_T$ , reduces from  $21 \times 10^{-6} \text{ K}^{-1}$  at 8.4 hours of concrete age to  $12 \times 10^{-6} \text{ K}^{-1}$  at 16.4 hours. That following, the coefficient remains constant. [353, p. 15] also reports that the coefficient at very early ages differs from the one of mature concrete. The variation of the coefficient must relate to the continuous change in share of solids, fluids, and gases in mass per unit volume.

A design value of  $\alpha_T = 10 \times 10^{-6} \text{ K}^{-1}$  is valid for hardened normal strength and high strength concrete ([121, p. 94]). [353, p. 15] has applied this value to his investigations on restrained hardening concrete. As well as [388, p. 43] did to a rough calculation of the thermal strain of a concrete sample cooling off. Note that [210, p. 1053] and [368, p. 841] have the coefficient assumed being constant with time for their considerations simulating the behaviour of shotcrete.

For a thermal load, the elastic strain component results to ([68, p. 62])

$$\Delta \varepsilon_{el,T}(t) = \Delta T \cdot \alpha_T(t); \tag{4.2}$$

with

 $\Delta \varepsilon_{el,T}(t)$  elastic strain increment (or decrement) due to thermal load [m/m],

 $\Delta T$  change of temperature (heating or cooling) [K],

 $\alpha_T(t)$  coefficient of thermal expansion (or contraction) at the moment of loading [K<sup>-1</sup>].

The strain increment (or decrement) depends on the age of the concrete—indicated by the term (t)—, as the concrete's coefficient of thermal expansion changes with the curing level if not set constant.

#### **Empirical approximation**

Often, only the part of the thermal strain is considered that the hydration process causes. The effect of temperature changes in the surrounding (i.e., tunnel and rock mass) is then neglected.

Schubert (1988; [358]) proposes an equation he got by fitting of laboratory data. He himself states that the fitted development may be valid qualitatively but needs to be adjusted to at site conditions. The equation depends just on the concrete age, t. Note that the equation accounts only for thermal strain within the first days after the concrete has started to set (cf. Fig. 2 in the reference). [358, p. 151]

Schütz et al. (2011; [368]) adopted the approach by [358] (cf. previous paragraph) and substituted constant fitting values with six parameters: the coefficient of thermal expansion,  $\alpha_{th}$ ; the maximum increase in temperature above the ambient environmental temperature in the tunnel,  $\Delta T_{max}$ , that occurs after shotcrete installation at the time  $t_{max}$ ; the time at which the effect of the hydration on the temperature has ended,  $t_{zero}$ ; and  $A_t$  and  $C_t$  which both depend on  $t_{max}$  and  $t_{zero}$ . They further assume a constant temperature distribution across the thickness

of the shotcrete body and  $\alpha_{th} = \text{constant}$ . The implementation has been validated using data from [173]. For calibrated model parameters, refer to Tab. 4 in the reference. [368, p. 841ff]

Meschke (1996; [260]), in contrast, considers the thermal strain by a formulation that is equivalent to Eq. 4.2. Input parameters are the temperature,  $\theta$ , the reference temperature,  $\theta_0$ , and the coefficient of thermal expansion,  $\alpha^{\theta}$ . [260, p. 3129]

Neither Schädlich and Schweiger (2014; [348]) nor Neuner et al. (2017; [276]) account for thermal strain separately. However, [276, p. 3], in particular, state that the deformation of unsealed specimens during ordinary shrinkage tests comprises shrinkage strain and thermal strain. The hydration process causes the latter. And at ordinary creep tests, shrinkage strain, thermal strain, and creep strain develop. Although not explicitly stated in any of the two publications, it must be assumed that they concluded to have the thermal strain stemming from the hydration process considered with their formulation of the development of shrinkage strain and with related fittings. Then, however, the question arises whether [358] and [368] have fitted their formulation of the development of shrinkage strain (cf. p. 56) to data that has been corrected prior to fitting by subtracting the thermal strain.

#### 4.6.3 Shrinkage (delayed) strain

The European standard "Eurocode 2: Design of concrete structures" ([20, p. 32]) and the "Guide for Modeling and Calculating Shrinkage and Creep in Hardened Concrete" by the American Concrete Institute ([5, p. 4f]) distinguish between the two most important shrinkage components, namely

- the autogenous shrinkage and
- the drying shrinkage.

The development of both components depends on time but not on external mechanical loading<sup>13</sup>, and is controlled mainly by the ambient air humidity, the size of the concrete structure, and the concrete's composition ([20, p. 30]; cf. Fig. 4.4). Shrinkage causes a shortening of the structure's dimensions and the volume decreases ([368, p. 840]). Depending on whether shrinkage develops in an unrestrained or restrained setting, either compressive strain<sup>14</sup> (negative; cf. Fig. 4.4) or tensile strain (positive) is introduced.

Compared to cast concrete, shrinkage of tunnel linings made of shotcrete is more pronounced because of "less aggregate content and higher water-cement ratio" ([18] in [347, p. 39]). <sup>15</sup> However, to which amount shrinkage sums up can vary strongly along the lining circumference depending on the moist conditions. From measurements in a tunnel section of a subway in Vienna, [128, p. 84] report the maximum shrinkage being at the tunnel roof, whereas it is only 50% at the side wall and negligible small at the invert.

 $<sup>^{13}</sup>$ [260, p. 3129] cites several publications all stating that shrinkage is independent of the acting stresses. However, he also cites [25] who disagrees with this.

<sup>&</sup>lt;sup>14</sup>The term *compressive* is misleading here because no mechanical compressive loading must be present to have the concrete element shrink. The term refers to the value sign rather than on the action causing the strain.

<sup>&</sup>lt;sup>15</sup>The cited statement is dubious since shotcrete usually features a lower water-cement ratio than conventional concrete. [174, Tab. 4–5, p. 7] cites ratios of 0.3 . . . 0.65 from standards and guidelines for shotcrete. [225, p. 61] recommends keeping the ratio below 0.5. In contrast, for standard concrete, usual upper thresholds range from 0.45 to 0.75 (cf. [37, Tab. 2, p. 1]). Anyway, [5, p. 6] states that for concrete with a water-cement ratio of less than 0.4 autogenous shrinkage contributes significantly to shrinkage strain. And according to [121, p. 92], drying shrinkage increases but autogenous shrinkage decreases with increasing water-cement ratio. Thus, one must differentiate between the types of shrinkage (cf. next subsections).

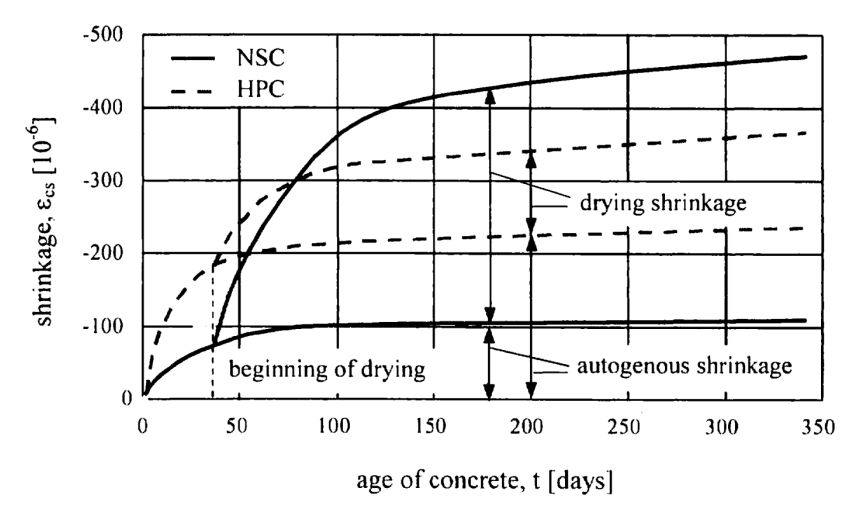


Figure 4.4: Development of autogenous and drying shrinkage with time in normal-strength concrete (NSC) and in high-performance concrete (HPC) (from [120, Fig. 3.1-13, p. 43]).  $\varepsilon_{cs}$  ... total shrinkage (in metre per metre).

#### Autogenous shrinkage

Autogenous<sup>16</sup> shrinkage (also termed basic shrinkage; cf. [121, p. 92]) results from two phenomena: hydration shrinkage (also termed chemical shrinkage; cf. [401, p. 785]) and capillary shrinkage (cf. [155, p. 693]). The former is due to volume reduction as the cement hydrates. The reason for the latter is that capillary traction between the liquid and the gaseous phase saturating the porous space increases and compresses the skeleton (i.e., the compound shrinks) ([401, p. 788]) in case free water is *lost*.

Generally, loss of water results if free water is consumed by the hydration reaction ([401, p. 788]) or evaporates ([388, p. 37]). By definition, autogenous shrinkage is determined under closed conditions, meaning that any fluid exchange with the surrounding exterior is prevented ([168] in [369, p. 149]). Shrinkage related to water loss due to evaporation is considered by drying shrinkage (cf. next subsection).

According to [279] (cited in [388, p. 37]), capillary shrinkage is possible only as long as the concrete is still plastic and takes place before the cement paste sets ([4, p. 3]). Capillary shrinkage is, therefore, also known as plastic shrinkage (cf. [326, p. 304], [388, p. 37]). In case the concrete specimen is placed underwater, capillary traction does not increase but rather decreases and causes swelling ([202] in [4, p. 3]).

Autogenous shrinkage is most prominent in the curing period and its development (temporal amount, effective period) strongly depends on the temperature and, therefore, also on the size of the concrete structure which controls the heat storage capacity ([353, p. 22]). However, the asymptotic value is independent of temperature variations ([401, p. 791]). According to ([353, p. 22]), a part of the shrinkage already takes places before strength develops and does not affect the stress regime within the structure.

Compared to drying shrinkage, autogenous shrinkage approaches its ultimate value relatively soon (cf. Fig. 4.4). According to [401, p. 791], autogenous shrinkage takes approx. 2 ... 3 months.

Autogenous shrinkage decreases with increasing water-cement ratio and increases with increasing cement paste content ([121, p. 92]).

For further reading on autogenous shrinkage, refer, for example, to [230, 385].

 $<sup>^{16}</sup>$ Autogenous: Produced independently of external influence or aid. [259]

#### Drying shrinkage

Drying shrinkage is caused by diffusion of chemically unbounded water ([353, p. 20]), occurs in the hardened cement paste as soon as this *free* water in large voids and capillary pores is absorbed, and takes place over several years ([388, p. 38ff]; cf. Fig. 4.4). Note that for drying shrinkage also the capillary traction is in charge, but the origin of water loss is different.

Diffusion is a natural process where a concentration difference between two adjacent substances (e.g., concrete structure and surrounding air) is levelled out. Hence, the development (amount, effective period) of drying shrinkage depends predominantly on the size of the concrete structure—the thicker the structure, the more chemically unbounded water exists and the more time it takes for water at the structure's core to diffuse to the structure's boundary—and on the ambient air humidity determining the (initial) concentration difference. The rate of the drying process decreases disproportionately to the size of the structure ([353, p. 21]).

As drying shrinkage develops in the hardened cement paste, all factors increasing the final quantity of hardened cement paste will yield to increased drying shrinkage (cf. [121, p. 92]). Such a factor can be, for example, an increased cement content ([279] in [388, p. 38]). Using plasticisers or other water-reducing admixtures requires a higher share of cement in the mix. Large stiff aggregates impede shrinkage. Hence, a finer grading curve of the aggregates indirectly boosts drying shrinkage in two ways. First, shotcrete with more content of fine aggregates needs relatively more cement. And second, the shotcrete has less big stiff aggregates, which reduces the restraining effect of such ([313] in [388, p. 39]). The same applies to the water-cement ratio. An increased ratio leads to a reduced proportion of aggregates and to more shrinkage (cf. [121, p. 92]). [388, p. 38f]

By re-wetting the concrete it will swell. This can recover a part of the long-term drying shrinkage. [168, p. 32]

#### Carbonation shrinkage

Carbonation shrinkage is irreversible and starts at the surfaces of concrete structures due to the reaction of carbonic acid (from carbon dioxide and air) with hydrates of the hardened cement paste ([388, p. 41], [4, p. 3]).

None of the guidelines considered (i.e., [5, 20, 121]) deal with carbonation shrinkage. Thus, its negligible share of total shrinkage is assumed. [284] (cited in [388, p. 41]) reports typical values for the depth of carbonation of 2 to 3 mm after six months. This rate is too low to contribute significantly in the early-age volumetric shrinkage. In particular, because the carbonation process starts in the surface layers.

#### **Empirical approximation**

Schubert (1988; [358]) approximates shrinkage with the hyperbolic equation by [2]. Schädlich and Schweiger (2014; [348]) and Schütz et al. (2011; [368]) use the same equation but refer to [3]. The equation considers the ultimate shrinkage strain at infinite time,  $\varepsilon_{\infty}^{sh}$ , the age of the shotcrete, t, and the constant B (in time units). [348] substitute B with  $t_{50}^{sh}$  which refers to the time when 50% of shrinkage has occurred. According to [3, p. 7], the equation covers autogenous, drying, and carbonation shrinkage. [368] use data summarised in [387] to validate their implementation. For calibrated model parameters, refer to Tab. 3 in [368, p. 843]. [348] validate their implementation with data from a shrinkage test on a polymer-modified shotcrete reported in [309, Fig. 7b, p. 7] (cf. [347, p. 39f]). [265] reports in detail about this shotcrete. Tab. 7 in [347, p. 42] lists recommended

values for the model parameters:  $\varepsilon_{\infty}^{sh} = [-0.0005; -0.0015]$  (dimensionless),  $t_{50}^{sh} = [28; 100]$  (in days).

Both Meschke (1996; [260]) and Neuner et al. (2017; [276]) make use of the semi-empirical shrinkage law by [28]. The equation considers the ultimate shrinkage strain at infinite time and at zero per cent humidity,  $\varepsilon_{\infty}^{sh}$ , the age of the shotcrete, t, the age of the shotcrete at the start of drying,  $t_0$ , the effective thickness of the shotcrete body,  $d_{eff}$ , and the function  $k_h$  for the humidity ([260, p. 3129]). [276, p. 14f] validate their implementation with data from [271]. Because not stated otherwise, it must be assumed that the data stems from shrinkage tests on unsealed shotcrete specimens. Thus, shrinkage strain comprises the autogenous and the drying part.

Note one important fact: At shrinkage tests on unsealed specimens, next to autogenous shrinkage and drying shrinkage, also the thermal strain due to the hydration heat contributes to the measured total strain. [276, p. 3]

#### 4.6.4 Creep (delayed) strain

The development of creep strain starts after the initial loading and increases with time under sustained constant load ([4, p. 3]). Creep results in an overall decrease in volume ([388, p. 46]). The cause of creep strain is not fully clarified yet ([4, p. 4], [389, p. 50]) but is controlled predominantly by the properties of the hydrated cement paste ([353, p. 26], [389, p. 50]).

Short-term creep relates to the movement of capillary water within the cement matrix upon load ([332] and [421] in [370, p. 284]; [153, p. 12] terms this *consolidation*). Here, thermodynamic forces, which depend on the stress state, determine the rate of water diffusion (cf. [399] in [370, p. 285]).

Long-term creep relates to changes in the micro-structure of the calcium silicate hydrate (C-S-H) phase ([30] in [370, p. 284]; cf. [353, p. 26]). Because of the external load, microbonds (microprestresses) created during the hydration process break locally and reform. This relaxation or dislocation-type mechanism is termed viscous flow (comprising viscous flow strain and viscous slip). [32] have proposed the theory (cf. Subsection 'Concept of the microprestress force' on p. 60). At a constant load, the potential for viscous flow is limited and the rate of viscous flow decreases continuously. [370, p. 284ff]

According to [141] (cited in [353, p. 26]), also intergranular sliding and microcracking contribute to the viscous deformation.

Note that some creep strains are recoverable (i.e., viscoelastic creep strain) while others are irrecoverable (i.e., viscoplastic creep strain). The former comprises, for example, the delayed elastic strain because of the interaction between the cement matrix and the aggregates. The latter results because of, for example, microcracking, crystal failure, and sliding within the micropores of the cement gel ([370, p. 284]). [4, p. 4f]

As the age of the concrete controls the development of all creep mechanisms (e.g., strength and stiffness increase with age yielding to less delayed elastic and plastic strain; cf. Section 4.6.5 on p. 60 and Section 4.6.6 on p. 62), creep strain relate to the amount of the initial loading and of any loading increment or decrement, and to the moment the loading situation changes. However, [10, p. D-50f] states that the utilisation of the concrete and the loading duration determine the creep rate significantly more than the concrete age.

Considering the boundary conditions, Fig. 4.1 (p. 48) divides creep into two main components: basic creep (non-drying creep) and drying creep. The basic creep is the sum of all creep strain components that develop at a constant moisture state of the concrete (no moisture losses or gains;

no moisture movement through the material) and are, therefore, independent from the size and shape of the structure ([4, p. 3]). Resulting strains are irrecoverable ([31] in [154, p. 27]). Drying creep develops because of changes in the moisture content and the development of a moisture potential within the concrete structure, which causes the capillary water to move (moisture diffusion). Similarly to drying shrinkage (cf. Section 4.6.3 on p. 54), drying creep depends mainly on the structure's size and shape which determine the initial moisture content, the surface area subjected to the surrounding media where the drying process starts, and the volume for which the humidity equilibrium must be found. According to [173] (cited in [388, p. 47]), it decreases with increasing size of the structure. Probably because a bigger structure needs more time for balancing meanwhile the shotcrete hardens.

In case the concrete is subjected to sustained load, both drying shrinkage and drying creep develop. Hence, it is difficult to quantify their share of the total strain ([388, p. 44]). In general, it is assumed that creep develops independently from shrinkage. Shrinkage coefficients are separately determined with shrinkage tests (recording of the change in strain with time because of drying; the sample is not subjected to any load). However, this assumption is probably wrong as creep and shrinkage are both linked to movement of water ([280] in [388, p. 44]).

Creep strain and creep strain rates increase ([388, p. 46])

- the earlier the concrete is loaded resulting in a higher utilisation;
- with increasing magnitude of load<sup>17</sup>, resulting in a higher utilisation; creep is proportional to an uniaxial load at low stress levels of  $< 0.4 f_c$  (cf. limit of proportionality in Section 4.9 on p. 66)<sup>18</sup>; above this level, the creep rate increases; progressive creep and, eventually, failure at stress levels of  $> 0.8 f_c$  ([1]);<sup>19</sup>
- with decreasing relative humidity as a lower humidity speeds up the drying process.

With the shotcrete ageing, the creep rate reduces (cf. [348, p. 103]), probably because the amount of solid hydrates already formed increases and this slows down the movement and diffusion of the remaining free water (cf. Section 4.1 on p. 47) and increases the restraining effects.

With regard to the shotcrete mix and the properties of its constituents, the cement content, the aggregates, and the porosity of the cement paste affect creep directly. Creep increases with increasing concrete porosity ([279] in [295, p. 2]) because it allows for more water movement. Substituting cement to some extent with micro-silica reduces the porosity ([388, p. 47]). Creep also increases with increasing cement content (e.g., [173] and [280] in [388, p. 46]), probably as a higher cement content yields to higher hydration temperature which speeds up the drying process. However, a higher cement content—assuming a constant water content—implies a reduced water-cement ratio with which the concrete develops a higher strength as fewer voids remain after the hydration process ([388, p. 20]). A higher strength leads to a lower utilisation and, therefore, to less creep.

Aggregates embedded within the cement paste hamper the development of creep (as for shrinkage too: cf. Section 4.6.3 on p. 54; and for reinforcement: cf. [98] in [295, p. 2]). Bigger and stiffer aggregates decrease the total amount of creep. Unfavourable aggregate shape may

<sup>&</sup>lt;sup>17</sup>Recent tests showed that the relation between creep strain and load level can also be negative (i.e., more strain at lower load levels) (cf. [124] in [153, p. 17]).

<sup>&</sup>lt;sup>18</sup>Note that the limit of proportionality differs for compressive and tensile loading (cf. [153, p. 17]). For differences between creep under compression and creep under tension, refer to, e.g., [99, p. 18f].

<sup>&</sup>lt;sup>19</sup>Related to the level of (constant) loading, creep can be divided into three stages ([153, p. 8]): (1) primary creep with a decreasing rate; (2) secondary creep with a relatively uniform rate; (3) tertiary creep with an (disproportionately) increasing rate. The phases relate to a constant load and temperature state ([333, p. 173]). Because the concrete's strength increases with its age, it can sustain higher loads at later stages (cf. [10, p. D-34f]).

introduce stress concentrations promoting microcracking and, thus, also creep effects ([235] in [153, p. 14]). [388, p. 47]

All other parameters (e.g., water-cement ratio, cement type, amount and type of admixtures and additions) affect the development of creep strain only indirect as they determine the development of the concrete's strength and, hence, the strength-stress ratio (or utilisation). [388, p. 47]

#### Relaxation

Creep is by definition the increase in strain with time under a sustained stress ([280] in [295, p. 1]). Relaxation, on the other hand, is the decrease in stress with time under constant strain ([280] in [388, p. 44]). If high loads subject the shotcrete prior to relaxation, relaxation then takes place faster and to a higher amount ([129, p. F-60]).

In reality, pure relaxation having a fully constrained deformation state is rare. The same applies to creep. When subjected by a restraint stress, deformation restraints are introduced. The latter partly impedes the development of creep strain. Thus, usually creep and relaxation are active simultaneously and depend on each other. Relaxation reduces the stress level. At lower stresses, less creep develops. [153, p. 21]

#### **Empirical approximation**

The rate of flow method ([107]) used by Schubert (1988; [358]) distinguishes between reversible and irreversible creep stain. The reversible part is split into short-term and long-term creep. Each requires an ultimate creep constant  $C_{d_{\infty}}$  and a creep rate constant Q. The irreversible part is adjusted with an age-related creep function  $C_{(t)}$ . Those parameters, the reversible strain at the previous time step, and the stress determine the resulting creep at a particular moment. To account for loadings of  $> 0.5 f_c$  and the related non-linear dependency of the creep rate on the stresses ([325] in [358, p. 151]), he (but also [128, p. 81]) adds an exponential term to the primary creep function  $C_{(t)}$ . [358, p. 150f]

Schädlich and Schweiger (2014; [348]) use a viscoelastic approach. It requires, for example, a creep factor,  $\varphi^{cr}$ , the stress, the time at the start of the loading,  $t_0$ , and the time until 50% of creep strains have developed,  $t_{50}^{cr}$ . Up to a shotcrete utilisation of 45% in compression, the creep factor is a constant. Above, it is replaced by the function  $\varphi_k^{cr}$  by [110] which considers the utilisation. They validate their implementation with data from [10]. Tab. 7 in [347, p. 42] lists recommended values for the model parameters, e.g.:  $t_{50}^{cr} = [1; 5]$  (in days). [348, p. 107f]

To consider creep and relaxation, Schütz et al. (2011; [368]) transferred the uniaxial time-dependent Newton dashpot into the general stress space. The resulting implementation requires, for example, the creep potential,  $P^{cr}$ , the applied stress, the initial age of the shotcrete upon loading,  $t_0$ , and the time-dependent viscosity function  $\eta(t)$ . For the validation, they use data from [206]. For calibrated model parameters, refer to Tab. 2 in the reference. [368, p. 840ff]

Meschke (1996; [260]) uses a Duvaut-Lions type viscoplastic formulation published by [374]. Here, creep strain can develop only in the plastic regime. Next to the stress, the formulation requires, for example, the viscosity parameter  $\eta^*$ . Data from [173] was used for validation ([261, p. 3150ff]). [260, p. 3133f], [276, p. 9f]

Neuner et al. (2017; [276]) applied a modified version of the solidification theory by [29]. The theory was transferred into the effective stress space. It distinguishes between viscoelastic strain and flow strain, among others. Both depend, for example, on the stress and the utilisation of the shotcrete. In the formulation of the viscoelastic strain, the parameter v(t) accounts for the

development of the load bearing volume fraction of the hydrated material. Data from [271] is used for the validation. [276, p. 3, 15ff]

Note one important fact: At creep tests on unsealed specimens, next to basic creep and drying creep, also autogenous shrinkage, drying shrinkage, and thermal strain contribute to the measured total strain. Thus, separate shrinkage tests on unsealed specimens are required to determine creep strain. [276, p. 3]

#### Concept of the microprestress force

To allow for a description of the microstructural processes determining long-term creep, [32] introduced the microprestress solidification theory. In this theory, the idealised C-S-H layers comprise sheets (cf. Fig. 4.5A and the building blocks in Fig. 4.5B). Note the water molecules in the interlayer region. Between those sheets, microprestress forces act. Resulting bonds are disordered and unstable. The pressure by the water molecules contributes disjoining the sheets but is counterbalanced by the existing bonds. Now, if the stresses apply to the concrete on the macroscale, bonds may break locally. This leads to slip of sheets relative to each other which, on the macroscale, is observed as long-term creep. The sliding of the sheets results in a reduction (relaxation) of the microprestress forces. In [154], the process described here is referred to as dislocation-like sliding in hydrates. [154, p. 10ff]

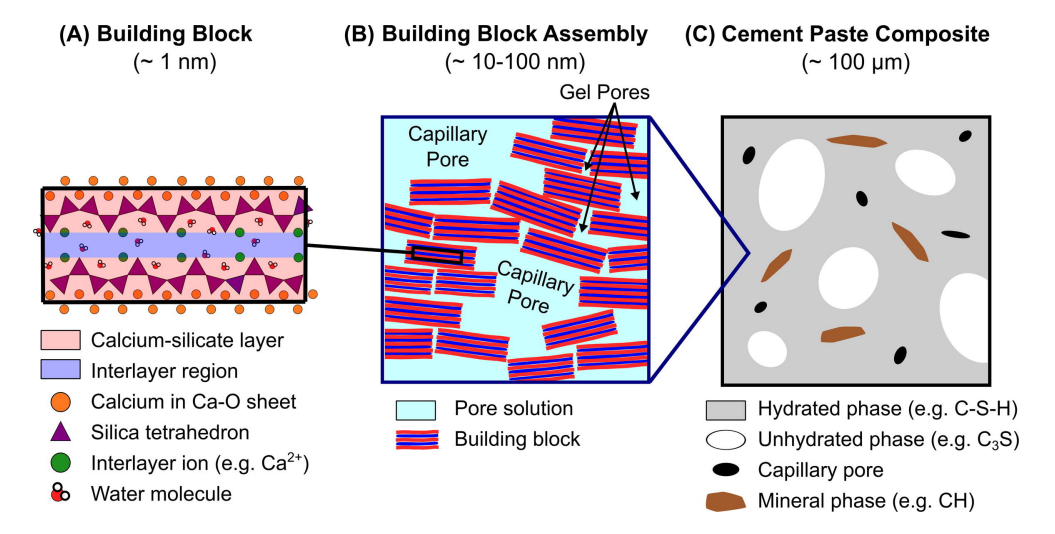


Figure 4.5: A multiscale perspective for cement paste materials (from [296, Fig. 1, p. 15]). (A) Building blocks describe the fundamental atomic interactions of the hydrated phase. (B) At larger scales, the hydrated phase is composed of an assembly of building blocks that form larger structures resulting in a hierarchical pore network. (C) The hydrated phase is intermixed with pores and mineral and unhydrated phases to form a cement paste composite at the microscale.

#### 4.6.5 Plastic (instantaneous) strain

To account for consistency in the description of the individual strain components, the term plastic must not be equated with the term irreversible (or irrecoverable).

Irreversible strain cannot be undone upon unloading (or load reversal). Here, unloading not only relates to a decrease in the level of mechanical stress applied externally to the concrete volume. It also relates to thermal loading and to other changes in the field or boundary conditions (e.g., change in the humidity). Some of this irreversible strain is a consequence of the ageing of the concrete (cf. Section 4.6.6).

It is irreversible because of two effects of which both stem from the change in the share of the constituents of the ageing concrete (more fluids, fewer solids  $\rightarrow$  fewer fluids, more solids):

- 1. As the share of fluids decreases, shear stresses introduced by the unloading (or load reversal) do result in less viscous flow. Instead, solids cope with those shear stresses and transfer them across solid-solid contacts. Note that macroscopically, viscous flow upon unloading can be (falsely) interpreted as elastic strain.
- 2. As the share of solids increases, solids more and more impede fluid flow and diffusion.

Strain components affected are the elastic, thermal elastic, shrinkage, and creep strain. As long as the concrete has not reached its final state of maturity, some of the elastic and thermal elastic strain remain irrecoverable. As for the shrinkage and creep strain, the concrete still comprises some free water even if it has fully hydrated (i.e., excess water) and more water can be introduced by re-wetting it. This allows for reversing some of the previous shrinkage or creep strain. However, at a hardened concrete, the strain rate is probably that small that strain reversal is non-existent from a practical engineering point of view.

Upon loading, the concrete compacts (or consolidates) and constituents are rearranged ([10, p. D-4, D-28ff]). This is more distinct in case the concrete is young. And, since viscous creep effects take place, also microcracks develop (or rather microbonds are destroyed; cf. Section 4.6.4 on p. 57). All resulting in (mostly) irreversible strain. In particular, the microcracks relating to creep may be also referred to as (visco-)plastic strain.

However, here, plastic strain as a separate component of the strain history of a loaded concrete specimen refers to irreversible deformation of the skeleton<sup>20</sup> (cf., e.g., [158, p. 2104], [402, p. 1127]). It also results in microcracks, but those cracks develop instantaneously rather than gradually as of those related to (viscous) creep. They are an immediate consequence of an overloading of the specimen; either in compression or in tension. This overload can be because of mechanical stresses applied externally. But it can be also because of restraints (cf. Section 4.5 on p. 50) combined with tensile strains introduced by shrinkage or by thermal contraction (cf. [156, p. 709], [157, p. 295f]). Note that shrinkage and creep (or relaxation) can reduce a critical compressive stress state.

Plastic strain develops also before the material reaches its peak strength ([348, p. 103]). Consider here the limit of proportionality described in Section 4.9 (p. 66) below which plastic strains are negligible. With the level of loading being above this threshold, the number and size of cracks will continuously increase, eventually leading to failure. The ageing of the concrete mentioned above indirectly also affects the amount of plastic strain because, with ageing, the strength develops (cf. [156, p. 707]). Thus, during hardening, of which the evolution rate depends on the temperature, any strength or strain thresholds continuously change (cf. Section 4.7). That, the moment of loading and, of course, also the loading magnitude strongly determine whether plastic strain results.

In the framework of numerical plasticity, hardening, softening, and flow rules aim to account for the non-linear stress-strain relationship. They need to consider the time-dependency of the strength and stiffness to allow for a proper modelling of the material behaviour in all of its states of maturity. (cf. [260, p. 3122])

 $<sup>^{20}</sup>$ The skeleton comprises the solid components of the compound (cf. Section 4.1 on p. 47).

<sup>&</sup>lt;sup>21</sup>The failure mechanisms involved depend on the stress state. It is cracking in pure tension and in mixed tension-compression states. But it is crushing in three-dimensional compression states. (cf. [260, p. 3122f])

#### **Empirical approximation**

The approach by Schubert (1988; [358]) is one-dimensional. Thus, it cannot account for plastic strain.

The model by Schädlich and Schweiger (2014; [348]) makes use of a Mohr-Coulomb and Rankine yield surface. On the compression side, they use the hardening and softening rules proposed by [368] (cf. next paragraph). On the tension side, the stress-strain relation is linear up to the tensile strength. Then a linear strain softening relation follows limited by a constant residual strength. [348, p. 103ff]

For the compression yield surface, Schütz et al. (2011; [368]) adopt the approach by [72]. And for the tension yield surface, it is a modified Rankine criterion proposed by [390]. The stress-strain relationship on the compressive side comprises a pre-peak quadratic (or parabolic) strain hardening part and two linear strain softening parts. The latter is limited by a constant residual strength. The tensile stress-strain relation is first parabolic (i.e., pre-peak strain hardening), followed by a linear or exponential strain softening part. Here, too, a constant residual strength limits the softening part. [368, p. 835ff]

Meschke (1996; [260]) applies the Drucker-Prager and the Rankine criterion. On the compression side, the stress-strain relation comprises a quadratic pre-peak part and a constant (perfectly plastic) post-peak strength (i.e., no softening). The post-peak softening part on the tension side is either linear or exponential. [260, p. 3123; Fig. 4, p. 3136]

The model by Neuner et al. (2017; [276]) bases on the one proposed by [134]. And the hardening/softening follows the approach by [258]. [276, p. 3ff]

#### 4.6.6 Irrecoverable strain due to ageing

As the hydration of the concrete (or shotcrete) proceeds, more and more solid phases substitute fluid and gaseous phases per unit volume of the composite (cf. Section 4.1 on p. 47). The concrete ages, continuously loses some of its initial ductility, stiffens (cf. Section 4.6.1 on p. 52), and its porosity decreases. As a result, movement of fluids within the composite, of which some shrinkage and creep effects originate (cf. Section 4.6.3 on p. 54 and Section 4.6.4 on p. 57, respectively), is increasingly impeded.

Now, imagine, even if all strain components listed above would be entirely recoverable (i.e., elastic), because of the ageing of the concrete, inelastic strain would result if the material is loaded at one moment and unloaded at any moment after. Literature terms it *ageing-induced strain* (cf., e.g., [261, p. 3147]).

This phenomenon affects all strain components except for the plastic strain, which is per se inelastic. Ageing-induced irrecoverable strains get small as soon as the concrete approaches its fully hydrated state.

#### 4.7 Peak strain

As in the previous paragraphs written, the concrete's ductility decreases with ageing. At a very early age, when not much hydrate mass has formed yet and the composite still allows for movement of the fluids, the ductility is high. Note that then most parts of the strain are plastic and irrecoverable upon unloading (cf. [10, p. D-36]). With proceeding hydration, the composite stiffens and the share of solids being more brittle increases. Accordingly, the peak strain—strain at peak strength—decreases as the concrete gets older (e.g., [371] in [368, p. 836]). It increases with increasing confining pressure ([64] in [348, p. 105]).

On the compression side, some reported concrete age related values are:

- 1-2 hours: -0.030... -0.040 m/m ([129] in [348, p. 106], [135] in [368, p. 836]);
- 8 hours: -0.005 m/m ([129] in [348, p. 106]);
- 24 hours: -0.002 m/m ([129] in [348, p. 106]).

The values comply with [47] who states that young shotcrete can sustain compressive strain of up to -0.005...-0.006 m/m with little spalling. Experiments suggest that peak strain remains relatively constant after 24 hours (cf. Fig. 8 in [347, p. 13]). Pay attention to the fact that [370, p. 289] estimated the characteristic (or retardation) time of short-term (viscoelastic) creep for a shotcrete material to be approx. 24 hours (cf. Subsection 'Diffusion of absorbed water—short-term creep' on p. 79).

On the tension side, [207] (cited in [368, p. 840]) report a range of peak strain values of 0.0002...0.0005 m/m. They also state that peak strain reduces significantly within the first hours after the application of the shotcrete. [63] (cited in [368, p. 840]) reports similarly low values with the tensile peak strain being 3% (at early stages) to 9% (at an age of 28 days) of the compressive peak strain.

## 4.8 Shotcrete strength

Section 4.2 (p. 47) briefly describes the origin of strength and stiffness increase with time. It relates to the continuous increase in the share of solids and bonds.

After two minutes, shotcrete already features a compressive strength of 0.1 to 0.2 MPa (cf. [289, p. 26]). The increase is first quasi-linear (cf. Section 4.2), but it is usually assumed that the rate then decreases exponentially. Anyway, there may be also phases with a lowered increase followed by a phase with an increased rate (cf. [208, p. 374]). The concrete mixture, the boundary conditions, and triggered chemophysical processes determine its development. Often, the peak strength is assumed to be reached after 28 days. This probably owns to several facts: (1) for standard concrete, the strength classes relate to strengths measured at samples with an age of 28 days (cf. [20, p. 27]); (2) for standard concrete with an age of over 28 days, the average strength is assumed constant (cf. [20, Eq. 3.2, p. 27]); (3) in standard cases, the long-term increase in strength is not of interest. However, having fittings to test data that reach the peak value asymptotically at 28 days may be wrong; at least for the today's shotcrete material. Consider here, for example, test results in [57, p. 23ff]. Fittings for the unreinforced shotcrete he tested, using a cement of class 42.5 and a water-cement ratio of 0.44, suggest a compressive strength of approximately 70 MPa at an age of 112 days, whereas it is approximately 61 MPa at 28 days.

Aggregates feature an inherent (or constant) strength and stiffness. The cement, superplasticisers (water-reducing admixtures), and accelerators are, however, reactive components of the shotcrete and their interaction influences the strength development ([352, p. 23]). According to [42, p. 37], the cement content, the water-cement ratio, and the temperature of the fresh concrete have the largest impact on the shotcrete's performance. Minor variations in one component's share, or the use of another type of component, results in different characteristics (e.g., reactivity) of the (hardening and hardened) shotcrete material (cf., e.g., [42, p. 32ff], [208, p. 351ff], [352, p. 26f]).

However, also the loading history during the hardening process affects the resulting performance. [10, p. D-11ff], for example, found out that if the shotcrete sample is loaded below the damage threshold while it cures, eventually, the sample develops a higher strength compared to

one which has not been loaded at all. He relates this phenomenon to consolidation; pore space gets smaller and this presses excess water out. Note that shotcrete material usually features an increased water content to increase pumpability ([388, p. 20]). The dependency on the loading or strain history makes it impossible to set the laboratory testing program up in a way so that all scenarios are considered. For example, to determine the change in the shotcrete's utilisation correctly in the laboratory requires two theoretically identical samples experiencing the same loading or strain history but tested at different moments (cf. [10, p. D-5]). Anyhow, referring to the shotcrete installed in the tunnel, the exact history is unknown prior to construction (or at all).

Usually, the lining is mainly in a biaxial state of stress (e.g., [203] in [158, p. 2106]). If it is a biaxial compressive state, the strength is up to 25% higher than under an uniaxial compressive state ([368, p. 835]). It is similar for the failure strain (cf. [20, p. 37]). Some models introduce a constant coefficient for the ratio of biaxial to uniaxial compressive strength,  $f_b/f_c$ , (e.g., 1.16 in [155, p. 698] and in [261, p. 3146]). This approach is valid only because, according to [63] (cited in [155, p. 698]), the chemical hardening is (approximately) isotropic.<sup>22</sup> Strengths develop with (approximately) the same rate (cf. [388, p. 25]). This means that—next to the ratio mentioned before—also following strength ratios remain constant during hardening ([155, p. 698]): ratio of uniaxial compressive yield to uniaxial peak compressive strength,  $f_{cy}/f_c$ , (e.g., 0.25 in [155, p. 698], and 0.1 in [277, Tab. 1, p. 6]); ratio of uniaxial tensile to uniaxial compressive strength,  $f_t/f_c$ , (e.g., 0.1 in [155, p. 698] and in [348, p. 104]). Those ratios may not be constant for all shotcrete ages or loading situations. For example, according to [21] (cited in [388, p. 155]), the ratio  $f_u/f_c$  is increased at an early age because of the shotcrete's high ductility. If the model applied neglects the strength increase in case of a biaxial (or multiaxial) compressive stress state, calculated utilisation ratios are on the conservative side. Anyway, as soon as one principal stress component is tensile, results may be on the unsafe side. Note that, according to [74] (cited in [388, p. 17, 29]), the presence of tensile stress reduces the compressive strength but also peak (and failure) principal compressive and tensile strains. Chapter 8 (p. 169) shows that the strain field in the shotcrete lining of a conventional tunnel drive can be quite non-uniform. All imaginable biaxial stress states seem possible. From pure compression or pure tension to any intermediate state. Making it even more difficult, tension softening affects the material strength in compression, and compression softening affects the strength in tension ([347, p. 7]).

#### **Empirical approximation**

When modelling shotcrete strength, its time-dependence should not remain unconsidered. Single-valued yield strengths (analytical considerations) or yield surfaces (numerical simulations) should develop with time (cf. [260, p. 3128], [368, p. 835]). Because compressive strength and tensile strength are not proportional to each other ([121, p. 87]), development formulations shall be independent of each other. Anyhow, often the tensile strength is set proportional to the compressive strength (cf. text above and below).

[365, p. 39f] highlight a problem which arises when following standards. If one considers, for example, the "Austrian Guideline for Sprayed Concrete" ([289, p. 26f, 92f]; cf. also [19, p. 12]) and the "fib Model Code for Concrete Structures" ([121, p. 87]), the former suggests compressive strength values for an age up to 24 hours (i.e., early age strength), whereas the latter provides an equation to calculate the strength up to an age of 28 days. [20, p. 27] cites the same equation,

 $<sup>^{22}</sup>$ Here, pure chemical hardening (i.e., strength growth) is addressed. It is not to be confused with strain hardening or softening. (cf. [402, p. 1130])

but highlights that for an age of below three days, tests are required to get more precise values. Thus, there is a gap of 48 hours between the age of 24 hours and of 72 hours. According to [365, p. 39f], in conventional tunnelling, the main part of stress redistributions takes place within this period.

In his publication, Schubert (1988; [358]) does not address the strength of shotcrete material. Schädlich and Schweiger (2014; [348]) use the formulation proposed by [68]. It requires the compressive strength at 28 days,  $f_{c,28}$ , and the time-dependent coefficient  $\beta_{cc}(t)$ . The latter depends on the shotcrete age, t, and on the coefficient s. In the original formulation, s is to be selected depending on the type of cement. In their formulation, they substituted s with the function  $s_{strength}$  which depends on the compressive strength at 1 day,  $f_{c,1}$ , and on  $f_{c,28}$ . A lower boundary is introduced with 0.5% of  $f_{c,28}$ . And for t > 28 days, the compressive strength is assumed constant. Because the formulation by [68] results in very low strength for  $t \lesssim 2$  hours, they cite an alternative approach: for the first 24 hours, use the early age strength by [19, 289]; then, the development follows the approach by [292], which depends on t,  $f_{c,1}$ , and  $f_{c,28}$ . For their implementation, they consider several ratios constant during the hardening process, e.g., (values in parentheses are recommendations by [347, Tab. 7, p. 42])

- uniaxial compressive yield stress to uniaxial peak compressive strength,  $f_{cy}/f_c$ , ([0.10; 0.25]; dimensionless);
- uniaxial residual compressive strength to uniaxial peak compressive strength,  $f_{c,r}/f_c$ , (0.1; dimensionless);
- uniaxial residual tensile strength to uniaxial peak tensile strength,  $f_{t,r}/f_t$ , (0; dimensionless);
- uniaxial peak tensile strength at 28 days to uniaxial peak compressive strength at 28 days,  $f_{t,28}/f_{c,28}$ , ([0.05; 0.10]; dimensionless).

Note that for the tensile strength, they generally make use of a constant ratio of, e.g.,  $f_t/f_c = 0.1$ . The implementation has been validated with data from [129]. [348, p. 104, 106]

Schütz et al. (2011; [368]) also use the approach by [68]. The relation of the coefficient s to the cement type remains untouched. They use the approach to approximate the development of the compressive and tensile strength with time. Values are set constant for t < 1 hour and for t > 28 days. Similar to [348], they also make use of some strength ratios set constant during hardening. Data from [371] was used for validation. Tab. 1 in the reference lists some calibrated model parameters. [368, p. 839, 842]

Meschke et al. (1996; [261]) make use of a formulation proposed by [288] to describe the development of the strength in the first 24 hours. It depends on the shotcrete age, t, and on the compressive strength on day one,  $f_{c,1}$ . For the development for t > 24 hours, they use an approach by [292]. Note that this approach is not the same as [348] use (cf. text above). Anyway, the formulation here requires t,  $f_{c,1}$ , and the compressive strength at 28 days,  $f_{c,28}$ . They relate the development of the tensile strength to the one of the compressive strength following [63, 292]. It is a non-linear relation with two coefficients only. They use data from [129] for validation. [261, p. 3150ff, 3161]

For the approximation of the development of the compressive strength, Neuner et al. (2017; [276]) adopt the approach by [261] formulated for the development of the Young's modulus (cf. Section 4.9). The second-order polynomial for the development of the strength in the first hours (here:  $t \leq 6$  hours) is modified by adding a residual coefficient. This ensures that the strength is non-zero for t = 0 (here: 1% of  $f_{c,28}$ ). Note that a monotonic growth in strength results only

if  $f_{c,1}/f_{c,28} \ge 0.16$ . They, too, consider some strength ratios constant during hardening; for example, the uniaxial peak tensile strength to the uniaxial peak compressive strength,  $f_t(t)/f_c(t)$ . For all constant strength ratios, they use the value resulting at 28 days. Data from [173] was used for validation. [276, p. 6, 13f]

## 4.9 Shotcrete deformability

Like for the shotcrete strength (cf. Section 4.8 on p. 63), the stiffness increases with time during the hardening process (cf. Section 4.2 on p. 47). In the capillary pores, hydration products grow, increase their volume, and, by that, stiffen the material's rigidity ([370, p. 284]).

The overall stiffness at a particular time is the sum of the inherent stiffness of the individual constituents of the concrete mix (e.g., aggregates, fluids) and viscoelastic effects ([353, p. 9]). The latter relates to recoverable creep strain (cf. p. 57). According to [63, 71] (cited in [388, p. 31]), the rate of increase is higher for the stiffness than for the strength.

As numerically investigated and described in [156] and discussed also by [388, p. 111f, 155], the deformation rate of the ground determines the importance of having the stiffness development modelled properly. If the ground deforms at a very low rate, the stiffness development of the shotcrete at early ages is of less importance. If the deformation rates are higher, it is more important. Consider here that not only the time-dependent (or creep) characteristics of the ground determine the deformation rate, but also the construction sequences of the tunnel drive and the advance rate of the individual headings (i.e., time-independent advance-related deformations). In this regard, it should not go unmentioned that the loading rate at shotcrete linings usually is much lower than at laboratory tests ([10, p. D-13f]). In that case, because load during the hardening can result in a higher shotcrete strength and stiffness (cf. p. 63), the shotcrete stiffness of the tunnel lining is lower than recorded in the laboratory.

Relating to the utilisation, up to the limit of proportionality, concrete behaves approximately like a linear viscoelastic material ([242, p. 384]). Because of the viscoelastic part, the state of strain depends on the time and loading history (cf. [242, p. 394]). Anyway, at unloading, if the concrete would not age, the body would return to its undeformed state; not instantaneously, but with time. Because of the ageing, some strain is irreversible (cf. Section 4.6.6 on p. 62). For concrete and shotcrete, published values for the limit of proportionality range from 30% to 60% of the uniaxial compressive strength: 30% ([370, p. 287f], [118] in [388, p. 110]), 30 ... 40% ([242, p. 384, 396], [388, p. 113]), <40% ([173] in [388, p. 46]), 40% ([153, p. 9]), 50% ([128, p. 81]), 40 ...60% ([10, p. D-42]). Published data suggests a variability of the threshold depending on the concrete age (cf. Fig. 2.10 in [388, p. 30]). This may explain the range of the threshold cited here.<sup>23</sup> Performing compression tests, the Young's modulus should be determined within a stress range below the limit of proportionality ([388, p. 31]). At a higher utilisation, the modulus of the virgin loading curve, for example, can be much lower and decreases with increasing utilisation (cf. Fig. E-7.4 and Fig. E-7.5 in [129, p. E-36]). Like for the Young's modulus of rock material (cf. Section 3.2.9 on p. 36), the definition of the Young's modulus (e.g., tangent or secant modulus, virgin loading or unloading-reloading loop) decides upon the resulting value. Consider that [315] (cited in [388, p. 34]) suggests a ratio of the unloading-reloading modulus to the modulus of the

<sup>&</sup>lt;sup>23</sup>The initial concrete mix is more a fluid than a solid. With the setting of the cement paste, solid hydrates form (cf. Section 4.2 on p. 47 and Section 4.7 on p. 62). The share of free (not yet combined) water decreases, whereas the share of solids increases. (Very) Early age concrete features a particular ductility allowing for viscous strain (some elastic, some plastic) without failure. This happens on the microscale. Macroscopically, this viscous strain may be falsely ascribed to microcracking. This problem contributes to the difficulty in determining the limit of proportionality.

virgin loading curve of 1.1 to 1.5; [10, Fig. D-19, p. D-30] reports an average value of 1.27.

For unreinforced concrete, the Young's moduli under compressive and tensile loading are similar ([388, p. 37]). However, for the latter, the limit of proportionality seems to be higher: 60% ([74] in [388, p. 22, 35]), up to the fifth percentile of the characteristic axial tensile strength of concrete,  $f_{ctk;0.05}$ , ([153, p. 9]), 90% ([118] in [368, p. 837]); note that the publications refer to mature concrete. The threshold probably also varies depending on the shotcrete age. According to [52] (cited in [388, p. 36]), under tension, the behaviour of unreinforced and reinforced shotcrete is similar, but the reinforcement makes the composite less brittle once the loading passes the yield limit.

#### 4.9.1 Poisson's ratio

According to experimental results, the Poisson's ratio,  $\nu$ , does not change significantly with time (i.e., with the degree of hydration) ([214] in [401, p. 787]). [155, p. 695] also report that the ratio may be considered constant at very early ages. However, other investigations show that it significantly changes with the shotcrete age and tends to reach an asymptotic value after a few days (cf. Fig. 2.12 in [388, p. 32]; the graph plots data from [21, 209]). Similarly, [353, p. 15] states for concrete that the ratio at very early ages notably differs from the ratio of mature concrete. The largest differences exist when comparing with the ratio before strength growth starts.

[388, Tab. 5.1, p. 110] declares a constant value of 0.2 a common value for the design of shotcrete linings in soft to blocky ground. [74] (cited in [388, Tab. 5.1, p. 110]) limits the use of this value to a shotcrete state being farther away from failure. It is further assumed that the elastic Poisson's ratios in the compressive and tensile regime are similar ([388, p. 37]).

The approach by Schubert (1988; [358]) is one-dimensional and does not require a Poisson's ratio. Schütz et al. (2011; [368, p. 839]) explicitly state that they set the Poisson's ratio constant. Schädlich and Schweiger (2016; [347, Tab. 7, p. 42]) recommend a value of 0.15 to 0.25. Meschke et al. (1996; [261, p. 3150]) used either 0.25 or 0.3 for their analyses.

#### 4.9.2 Empirical approximation

Schubert (1998; [358]) approximates the development of the Young's modulus, E(t), with a formulation proposed by [67]. It depends only on the shotcrete age, t, and the Young's modulus at 28 days,  $E_{28}$ . [358, p. 151]

Schädlich and Schweiger (2014; [348]) use the formulation proposed by [68, p. 51f]. However, instead of using the time-dependent coefficient  $\beta_E(t)$  suggested by the standard, they rather use the same coefficient  $\beta_{cc}(t)$  as for the formulation of the compressive strength (cf. p. 65). The resulting formulation depends on the shotcrete age, t, the Young's modulus at 28 days,  $E_{28}$ , and on the coefficient s. In the original formulation, the latter depends on the type of cement. In their formulation, they substituted s with the function  $s_{stiff}$  which depends on the Young's modulus at 1 day,  $E_1$ , and on  $E_{28}$ . Note that they consider the Young's modulus constant for t < 1 day and for t > 28 days. The formulation has been validated using data from [71]. For  $E_1/E_{28}$ , they recommend a value between 0.5 and 0.7 ([347, Tab. 7, p. 42]). [348, p. 106]

Schütz et al. (2011; [368]) use also the formulation proposed by [68, p. 52]. But in contrast to [348], they used the relating time-dependent coefficient  $\beta_E(t)$ . And they stick to the dependency of s on the type of cement. Here, too, the Young's modulus is set constant for t < 1 day and for t > 28 days. Data from [371] served for the validation. [368, p. 839, 842]

According to Meschke et al. (1996; [261]), the formulation they use to account for the time-dependent Young's modulus bases on the one given in [68]. However, the formulation is rather similar to the one [358] uses who refers to [67]. Anyway, they modified the formulation by introducing a second-order polynomial for the development of the Young's modulus in the first eight hours. They also set the Young's modulus constant for a shotcrete age of over 28 days. The final formulation depends on the concrete age, t, the Young's modulus at day one,  $E_1$ , the Young's modulus at 28 days,  $E_{28}$ , and on some constants. If  $E_1$  is unknown,  $E_1/E_{28} = 0.6$  is assumed. Data from [122, 173] are used to validate the formulation. Tab. 1 in the reference lists some values for  $E_1/E_{28}$ . [261, p. 3148ff, 3159f]

As mentioned already in Section 4.6.4 (p. 57), Neuner et al. (2017; [276]) utilise a modified version of the solidification theory by [29]. The volume function v(t) (cf. p. 59) describes also the development of the Young's modulus with time. It required a modification of v(t), as the development in the first hours did not yield satisfying results. The final implementation requires, for example, the shotcrete age, t, the Young's modulus at day one,  $E_1$ , and some coefficients. The validation was performed using data from [173]. [276, p. 6ff]

# Bibliography

- [1] Abler, P. Einflüsse auf das Verformungsverhalten von jungem Spritzbeton im Tunnelbau. Diploma thesis, University of Innsbruck, Innsbruck, Austria, 1992.
- [2] ACI. ACI Manual of Concrete Practice. Technical report, American Concrete Institute (ACI), 1978.
- [3] ACI Committee 209. 209R-92. Prediction of Creep, Shrinkage, and Temperature Effects in Concrete Structures. Technical report, American Concrete Institute (ACI), March 1992. Reapproved 1997.
- [4] ACI Committee 209. 209.1R-05. Report on Factors Affecting Shrinkage and Creep of Hardened Concrete. Technical report, American Concrete Institute (ACI), July 2005.
- [5] ACI Committee 209. 209.2R-08. Guide for Modeling and Calculating Shrinkage and Creep in Hardened Concrete. Technical report, American Concrete Institute (ACI), May 2008.
- [6] Acker, P. Comportement mécanique du béton: Apports de l'approche physico-chimique (Mechanical behavior of concrete: A physico-chemical approach). PhD thesis, Ecole Nationale des Ponts et Chaussées, Paris, France, 1988.
- [7] Acker, P. Micromechanical Analysis of Creep and Shrinkage Mechanisms. In Ulm, F.-J., Bažant, Z. P., and Wittmann, F. H., editors, Creep, Shrinkage and Durability Mechanics of Concrete and other Quasi-brittle Materials. Proceedings of the 6th International Conference CONCREEP@MIT, pages 15–26, Cambridge, USA, August 2001. Elsevier: Amsterdam.
- [8] Adhikary, D. P. Shortcomings in the standard continuum based implicit joint model of layered rocks. *Journal of Geology and Mining Research*, 2(2):23–28, May 2010.
- [9] Alber, M. and Kahraman, S. Predicting the uniaxial compressive strength and elastic modulus of a fault breccia from texture coefficient. *Rock Mechanics and Rock Engineering*, 42(1):117–127, January 2009.
- [10] Aldrian, W. Beitrag zum Materialverhalten von früh belastetem Spritzbeton. PhD thesis, Montanuniversität Leoben, Leoben, Austria, May 1991.
- [11] Allaby, M., editor. A Dictionary of Geology and Earth Sciences. Oxford University Press, 4th edition, January 2013.
- [12] Allmendinger, R. W. Stereonet, September 2020. URL https://www.rickallmendinger.net/stereonet. Last access: 26.09.2020.
- [13] Allmendinger, R. W., Cardozo, N., and Fisher, D. M. Structural Geology Algorithms: Vectors and Tensors. Cambridge University Press, December 2011.

BIBLIOGRAPHY 288 of 498

[14] ASTM. D5607-02. Standard Test Method for Performing Laboratory Direct Shear Strength Tests of Rock Specimens Under Constant Normal Force. Standard, 2002.

- [15] ASTM. D7012-10. Test Methods for Compressive Strength and Elastic Moduli of Intact Rock Core Specimens under Varying States of Stress and Temperatures. Standard, 2010.
- [16] Atkins, P., Jones, L., and Laverman, L. Chemical principles. W. H. Freeman and Company, 6th edition, 2013.
- [17] Atzl, G., Brandtner, M., Selan, V., and Moritz, B. Numerical analyses of deep tunnels driven through massive faults. In Schubert, W. and Kluckner, A., editors, *Proceedings of the ISRM Regional Symposium EUROCK 2015 & 64<sup>th</sup> Geomechanics Colloquium–Future Development of Rock Mechanics*, pages 877–882, Salzburg, Austria, October 2015. Austrian Society for Geomechanics.
- [18] Austin, S. A. and Robins, P. J., editors. Sprayed Concrete: Properties, Design and Application. Whittles Publishing, 1995.
- [19] Austrian Standards Institute. ÖNORM EN 14487-1-1:2006. Spritzbeton: Teil 1: Begriffe, Festlegungen und Konformität. Standard, May 2006.
- [20] Austrian Standards Institute. ÖNORM EN 1992-1-1:2015. Eurocode 2: Bemessung und Konstruktion von Stahlbeton- und Spannbetontragwerken Teil 1-1: Allgemeine Bemessungsregeln und Regeln für den Hochbau (konsolidierte Fassung). Standard, February 2015.
- [21] Aydan, O., Sezaki, M., and Kawamoto, T. Mechanical and numerical modelling of shotcrete. In Pande, G. N. and Pietruszczak, S., editors, Proceedings of the Fourth International Symposium on Numerical Models in Geomechanics (NUMOG IV), pages 757–764, Swansea, Wales, August 1992. Taylor & Francis, London.
- [22] Bandis, S. C., Lumsden, A. C., and Barton, N. R. Fundamentals of rock joint deformation. International Journal of Rock Mechanics and Mining Sciences & Geomechanics Abstracts, 20(6):249–268, December 1983.
- [23] Barbero, M., Bonini, M., and Borri-Brunetto, M. Numerical modelling of the mechanical behaviour of bimrock. In Ribeiro e Sousa, L., Olalla, C., and Grossmann, N., editors, Proceedings of the 11th Congress of the International Society for Rock Mechanics—The Second Half Century of Rock Mechanics, volume 1 & 2, pages 377–380, Lisbon, Portugal, July 2007. Taylor & Francis Group, London.
- [24] Barbero, M., Bonini, M., and Borri-Brunetto, M. Three-Dimensional Finite Element Simulations of Compression Tests on Bimrock. In Proceedings of the 12th International Conference of International Association for Computer Methods and Advances in Geomechanics (IACMAG), pages 631–637, Goa, India, October 2008.
- [25] Bažant, Z. P., editor. Mathematical Modelling of Creep and Shrinkage in Concrete. Wiley & Sons Ltd, New York, 1988.
- [26] Bažant, Z. P. Creep and thermal effects in concrete structures: a conceptus of some new developments. In Mang, H. A., Bicanic, N., and de Borst, R., editors, *Proceedings of the Int. Conf. EURO-C "Computational Modelling of Concrete Structures"*, pages 461–480, Swansea, Wales, 1994. Pineridge Press.

BIBLIOGRAPHY 289 of 498

[27] Bažant, Z. P. Materials Science of Concrete IV, chapter Creep and Damage in Concrete, pages 335–389. American Ceramic Society, Westerville, USA, 1995.

- [28] Bažant, Z. P. and Panula, L. Practical prediction of time-dependent deformations of concrete. *Matériaux et Constructions*, 11(5):317–328, September 1978.
- [29] Bažant, Z. P. and Prasannan, S. Solidification Theory for Concrete Creep. I: Formulation. Journal of Engineering Mechanics, 115(8):1691–1703, 1989.
- [30] Bažant, Z. P. and Wittmann, F. H., editors. Creep and Shrinkage in Concrete Structures. John Wiley & Sons Ltd, Chichester, 1982.
- [31] Bažant, Z. P., Hauggaard, A. B., and Baweja, S. Microprestress solidification theory for concrete creep. II: Algorithm and verification. *Journal of Engineering Mechanics*, 123(11): 1195–1201, November 1997.
- [32] Bažant, Z. P., Hauggaard, A. B., Baweja, S., and Ulm, F.-J. Microprestress solidification theory for concrete creep. I: Aging and drying effects. *Journal of Engineering Mechanics*, 123(11):1188–1194, 1997.
- [33] Bell, F. G. Engineering Properties of Soils and Rocks. Butterworth-Heinemann Ltd: Oxford, 3rd edition, 1992.
- [34] Benz, T., Vermeer, P. A., and Schwab, R. A small-strain overlay model. International Journal for Numerical and Analytical Methods in Geomechanics, 33(1):25–44, January 2009.
- [35] Benz, T. Small-strain stiffness of soils and its numerical consequences. PhD thesis, University of Stuttgart, 2007.
- [36] Bergmair, M., Harer, G., Riedmüller, G., and Stadlmann, T. Die Baugeologie des Galgenbergtunnels. Felsbau, 14(1):15–21, 1996.
- [37] Biscoping, M. and Kampen, R. Zusammensetzung von Normalbeton Mischungsberechnung, February 2017. URL https://mitglieder.vdz-online.de/fileadmin/gruppen/vdz/3LiteraturRecherche/Zementmerkblaetter/ZM\_B20\_2017\_2.pdf. Zement-Merkblatt Betontechnik B 20; last access: December 16th, 2022.
- [38] Bjureland, W., Johansson, F., Sjölander, A., Spross, J., and Larsson, S. Probability distributions of shotcrete parameters for reliability-based analyses of rock tunnel support. *Tunnelling and Underground Space Technology*, 87:15–26, May 2019.
- [39] Bjurström, S. Shear strength of hard rock joints reinforced by grouted untensioned bolts. In Proceedings of the 3rd Congress of the International Society for Rock Mechanics (ISRM), pages 1194–1199, Denver, Colorado, USA, September 1974.
- [40] Blair, T. C. and McPherson, J. G. Grain-size and textural classification of coarse sedimentary particles. *Journal of Sedimentary Research*, 69(1):6–19, January 1999.
- [41] Blümel, M. Personal communication, November 2020.
- [42] Boos, P. and Dietermann, M. Wet Shotcrete Performance—Laboratory Test Methods and influencing Factors in Practice. *Tunnel*, 29(6):31–41, 2010.

BIBLIOGRAPHY 290 of 498

[43] Bossart, P., Meier, P. M., Moeri, A., Trick, T., and Mayor, J.-C. Geological and hydraulic characterisation of the excavation disturbed zone in the Opalinus Clay of the Mont Terri Rock Laboratory. *Engineering Geology*, 66(1–2):19–38, October 2002.

- [44] Boumiz, A., Vernet, C., and Tenoudji, F. C. Mechanical properties of cement pastes and mortars at early ages. *Advanced Cement Based Materials*, 3(3-4):94–106, April 1996.
- [45] Brady, B. H. G. and Brown, E. T. Rock Mechanics for underground mining. Springer Netherlands, 3rd edition, 2004.
- [46] Brandtner, M. Numerical Analysis of Fault Zones—Coming Closer to a Solution. In Schubert, W., Kluckner, A., and Pilgerstorfer, T., editors, *Proceedings of the Workshop "Characterization of Fault Zones" as part of the 62nd Geomechanics Colloquium*, pages 60–63, Salzburg, Austria, October 2013. Austrian Society for Geomechanics.
- [47] Brandtner, M. Personal communication, June 2020.
- [48] Brandtner, M. Personal communication, April 2022.
- [49] Brandtner, M. Personal communication, May 2022.
- [50] Brandtner, M. and Lenz, G. Checking the system behaviour using a numerical model. Geomechanics and Tunnelling, 10(4):353–365, August 2017.
- [51] Bray, J. W. Unpublished note. 1977.
- [52] BRITE-EURAM. BRE-CT92-0231. new Materials, Design and Construction Techniques for Underground Structures in Soft Rock and Clay Media. Technical report, Mott MacDonald Ltd (project coordinator), 1998. Research project funded by EU (programme: FP3-BRITE/EURAM 2).
- [53] Brodie, K., Fettes, D., Harte, B., and Schmid, R. Towards a unified nomenclature of metamorphic petrology: 5. structural terms including fault rock terms. PDF, November 2004. URL https://www.ugr.es/~agcasco/personal/IUGS/pdf-IUGS/scmr\_struc2\_structuraltermsincludingfaultrockterms.pdf. Recommendations by the IUGS Subcommission on the Systematics of Metamorphic Rocks. Last access: 07.01.2023.
- [54] Brosch, F.-J. and Pischinger, G. Small- to meso-scale brittle rock structures and the estimation of "paleostress" axes—A case study from the Koralm region (Styria/Carinthia). Austrian Journal of Earth Sciences, 107(2):37–59, 2014.
- [55] Brown, E. T. and Gonano, L. P. Improved compression test technique for soft rock. *Journal of the Geotechnical Engineering Division*, 100(2):196–199, 1974.
- [56] Brugg Kabel AG. Datasheet: BRUsens strain V3 (LLK-BSST V3 7.2 mm). Version: 2012/09/12 Rev. 02 TH. Technical report, Brugg, Switzerland, 2012.
- [57] Bryne, L. E. Time Dependent Material Properties of Shotcrete for Hard Rock Tunnelling. PhD thesis, KTH Royal Institute of Technology, Stockholm, Sweden, May 2014.
- [58] Buchmayer, F., Monsberger, C. M., and Lienhart, W. Advantages of tunnel monitoring using distributed fibre optic sensing. *Journal of Applied Geodesy*, 15(1):1–12, December 2020.

BIBLIOGRAPHY 291 of 498

[59] Budil, A. Längsverschiebungen beim Tunnelvortrieb. PhD thesis, Graz University of Technology, Graz, Austria, May 1996.

- [60] Bürgi, C. Cataclastic fault rocks in underground excavations A geological characterisation. Phd thesis, École Polytechnique Fédérale de Lausanne, Lausanne, Switzerland, 1999.
- [61] Burgstaller, M., Goricki, A., and Vanek, R. Semmering Base Tunnel new—Tender documents: Report on the geotechnical ground characterisation. Project document (in german), Austrian Federal Railways, April 2014.
- [62] Button, E. A. A Contribution to the Characterization of Phyllitic and Schistose Rock Masses for Tunnelling. PhD thesis, Graz University of Technology, Graz, Austria, 2004.
- [63] Byfors, J. Plain concrete at early ages. Technical report, Swedish Cement and Concrete Research Institute, Stockholm, Sweden, 1980.
- [64] Candappa, D. C., Sanjayan, J. G., and Setunge, S. Complete Triaxial Stress-Strain Curves of High-Strength Concrete. *Journal of Materials in Civil Engineering*, 13(3):209–215, June 2001.
- [65] Cardozo, N. and Allmendinger, R. W. Spherical projections with OSXStereonet. Computers & Geosciences, 51:193–205, February 2013.
- [66] Çengel, Y. A., Boles, M. A., and Kanoğlu, M. Thermodynamics: an engineering approach. McGraw-Hill Education, New York, USA, 9th edition, 2019.
- [67] CEB. International System of Unified Standard Codes of Practice for Structures—Volume 2: CEB-FIP Model Code for Concrete Structures. In CEB Bulletins d'information, number 124. Comité Euro-International du Béton (CEB), 1978.
- [68] CEB. CEB-FIP Model Code 90: Design Code. Technical report, Comité Euro-International du Béton (CEB), 1993.
- [69] Cervera, M., Oliver, J., and Prato, T. Thermo-Chemo-Mechanical Model for Concrete. I: Hydration and Aging. *Journal of Engineering Mechanics*, 125(9):1018–1027, September 1999.
- [70] Cervera, M., Oliver, J., and Prato, T. Thermo-Chemo-Mechanical Model for Concrete. II: Damage and Creep. Journal of Engineering Mechanics, 125(9):1028–1039, September 1999.
- [71] Chang, Y. Tunnel support with shotcrete in weak rock—a rock mechanics study. PhD thesis, KTH Royal Institute of Technology, Stockholm, Sweden, 1994.
- [72] Chen, A. C. T. and Chen, W.-F. Constitutive Relations for Concrete. *Journal of the Engineering Mechanics Division*, 101(4):465–481, August 1975.
- [73] Chen, G., Kemeny, J. M., and Harpalani, S. Fracture propagation and coalescence in marble plates with pre-cut notches under compression. In Myer, L. R., Cook, N. G. W., Goodman, R. E., and Tsang, S. F., editors, *Proceedings of the International Symposium on Fractured and Jointed Rock Masses*, pages 443–448, Lake Tahoe, California, USA, June 1992. A.A. Balkema.
- [74] Chen, W.-F. Plasticity in Reinforced Concrete. McGraw-Hill, New York, 1982.

BIBLIOGRAPHY 292 of 498

[75] Cheng, C. Influence of discontinuities on post-peak behavior of rock in uniaxial compressive test by numerical study. In Farag, A. A., editor, *Proceedings of the 2nd International Conference on Multimedia Technology (ICMT 2011)*, pages 6406–6409, Hangzhou, China, July 2011. Institute of Electrical and Electronics Engineers.

- [76] Cheng, Z. and Detournay, C. Plastic hardening model I: Implementation in FLAC3D. In Gómez, P., Detournay, C., Hart, R., and Nelson, M., editors, *Proceedings of the 4th Itasca Symposium on Applied Numerical Modeling*, pages 267–276, Lima, Perú, March 2016. Itasca International Inc., Minneapolis.
- [77] Cheng, Z. and Lucarelli, A. Plastic hardening model II: Calibration and validation. In Gómez, P., Detournay, C., Hart, R., and Nelson, M., editors, *Proceedings of the 4th Itasca Symposium on Applied Numerical Modeling*, pages 393–402, Lima, Perú, March 2016. Itasca International Inc., Minneapolis.
- [78] Codegone, G., Festa, A., and Dilek, Y. Formation of Taconic mélanges and broken formations in the Hamburg Klippe, Central Appalachian Orogenic Belt, Eastern Pennsylvania. Tectonophysics, 568-569:215–229, September 2012.
- [79] Coli, N., Berry, P., and Boldini, D. Analysis of the block-size distribution in the Shale-Limestone Chaotic Complex (Tuscany, Italy). In Wilson, S., Ewy, R., and Tutuncu, A., editors, Proceedings of the 42nd US Rock Mechanics Symposium and 2nd U.S.-Canada Rock Mechanics Symposium, pages 1–7, San Francisco, California, 29 June–2 July, 2008. American Rock Mechanics Association (ARMA): Alexandria. ARMA 08-233.
- [80] Coli, N., Boldini, D., and Bandini, A. Modeling of complex geological rock mixtures under triaxial testing conditions. In *Proceedings of the 2012 Regional Symposium of the International Society for Rock Mechanics (EUROCK 2012)—Rock Engineering and Technology for Sustainable Underground Construction*, pages 1–12, Stockholm, Sweden, May 2012.
- [81] Cook, N. G. W. The application of seismic techniques to problems in rock mechanics. International Journal of Rock Mechanics and Mining Sciences & Geomechanics Abstracts, 1(2):169–179, March 1964.
- [82] Cook, N. G. W. An experiment proving that dilatancy is a pervasive volumetric property of brittle rock loaded to failure. *Rock Mechanics*, 2(4):181–188, December 1970.
- [83] Cook, N. G. W., Hoek, E., Pretorius, J. P. G., Ortlepp, W. D., and Salamon, M. D. G. Rock mechanics applied to the study of rockbursts. *Journal of the South African Institute* of Mining and Metallurgy, 66:436–528, 1966.
- [84] Cordes, T., Weifner, T., Unteregger, D., and Bergmeister, K. Interaction between deep tunnel drives and an existing tunnel in fault zones-Modelling against reality. *Geomechanics* and Tunnelling, 12(6):641-650, December 2019.
- [85] Cornejo-Malm, G. Schwinden von Spritzbeton. Research report, ETH Zurich, 1995.
- [86] Coussy, O. Mechanics of Porous Continua. Wiley: Chichester, United Kingdom, 1995.
- [87] Coussy, O. Mechanics and physics of porous solids. John Wiley & Sons, Ltd: Chichester, United Kingdom, 1st edition, 2010.

BIBLIOGRAPHY 293 of 498

[88] Cowan, D. S. Structural styles in Mesozoic and Cenozoic mélanges in the western Cordillera of North America. *GSA Bulletin*, 96(4):451–462, April 1985.

- [89] Cudny, M. and Truty, A. Refinement of the Hardening Soil model within the small strain range. *Acta Geotechnica*, 15(8):2031–2051, March 2020.
- [90] Daller, J., Atzl, G., and Blümel, M. Festschrift zum 60. Geburtstag von Wulf Schubert, chapter Bestimmung von Gesteinskennwerten an Störungsmaterial, pages 50–58. Institute of Rock Mechanics and Tunnelling, Graz University of Technology, Graz, Austria, 2010.
- [91] Dassault Systèmes Simulia Corp. Abaqus/CAE 2017 documentation.
- [92] Davila Mendez, J. M. Displacements Analysis in Layered Rock Masses. PhD thesis, Graz University of Technology, Graz, Austria, January 2016.
- [93] Deere, D. U. Rock Mechanics in Engineering Practice, chapter Geological considerations, pages 1–20. Wiley, New York, 1968. Chapter 1.
- [94] Deere, D. U. and Miller, R. P. Engineering classification and index properties for intact rock. Technical report AFWL-TR-65-116, Air Force Weapons Laboratory, Kirtland Air Force Base, New Mexico, USA, December 1966.
- [95] Deutsche Gesellschaft für Geotechnik e.V. (DGGT). Empfehlungen des Arbeitskreises "Numerik in der Geotechnik"–EANG. Wilhelm Ernst & Sohn, Verlag für Architektur und technische Wissenschaften GmbH & Co. KG, Berlin, Germany, February 2014.
- [96] Dickmann, T. Personal communication, July 2021.
- [97] Diederichs, M. S., Carvalho, J. L., and Carter, T. G. A Modified Approach For Prediction of Strength And Post Yield Behaviour For High GSI Rockmasses In Strong, Brittle Ground. In Eberhardt, E., Stead, D., and Morrison, T., editors, Proceedings of the 1st Canada-US Rock Mechanics Symposium: Rock Mechanics: Meeting Society's Challenges and Demands, pages 249–257, Vancouver, Canada, April 2007. ARMA-07-031.
- [98] Ding, Y. Technologische Eigenschaften von jungem Stahlfaserbeton und Stahlfaserspritzbeton. PhD thesis, University of Innsbruck, Innsbruck, Austria, 1998.
- [99] Dorfmann, E. M. Zugkriechen von Beton in Abhängigkeit der Spannungsgeschichte. Master's thesis, Graz University of Technology, Graz, Austria, June 2017.
- [100] Eberhardt, E. Numerical modelling of three-dimension stress rotation ahead of an advancing tunnel face. *International Journal of Rock Mechanics and Mining Sciences*, 38(4):499–518, June 2001.
- [101] Eberly, D. Approximating an Ellipse by Circular Arcs, April 2016. URL https://www.geometrictools.com/Documentation/ApproximateEllipse.pdf. Last access: 26.09.2020.
- [102] Egger, P. Einfluss des Post-Failure Verhaltens von Fels auf den Tunnelausbau unter besonderer Berücksichtigung des Ankerausbaus. PhD thesis, Universität Karlsruhe, Karlsruhe, Germany, 1973.
- [103] Ekici, Z. Semmering Base Tunnel, construction lot SBT 1.1, tunnel Gloggnitz—Tender documents: Calculation values. Project document (in german), Austrian Federal Railways, 2014.

BIBLIOGRAPHY 294 of 498

[104] Engels, S., Wieselthaler, F., Pischinger, G., and Holzer, R. Semmering Base Tunnel, construction lot SBT 1.1, tunnel Gloggnitz, track 1—Engineering geological documentation. Project document (in german), Austrian Federal Railways, 2016.

- [105] Engels, S., Wieselthaler, F., and Holzer, R. Semmering Base Tunnel, construction lot SBT 1.1, tunnel Gloggnitz, track 1—Geotechnical horizontal and longitudinal section. Project document (in german), Austrian Federal Railways, 2017.
- [106] Engl, D. A., Fellin, W., and Zangerl, C. Scherfestigkeiten von Scherzonengesteinen—Ein Beitrag zur geotechnischen Bewertung von tektonischen Störungszonen und Gleitzonen von Massenbewegungen. Bulletin für Angewandte Geologie, 13(2):63–81, 2008.
- [107] England, G. L. and Illston, J. M. Methods of computing stress in concrete from a history of measured strain. *Civil Engineering and Public Works Review*, 60(1–3):513–517, 692–694, 846–847, April, May, June 1965.
- [108] Entfellner, M. Prediction of Displacements and Shotcrete Lining Utilization—Decision strategy for a timely application of ductile support systems in conventional tunnelling. Master's thesis, Graz University of Technology, Graz, Austria, August 2017.
- [109] Entfellner, M., Schubert, W., and Moritz, B. A. Early warning of overbreaks in tunnels. In Proceedings of the 2022 Regional Symposium of the International Society for Rock Mechanics (EUROCK 2022)–Rock and Fracture Mechanics in Rock Engineering and Mining, pages 1–8, Espoo, Finland, September 2022.
- [110] European Committee for Standardization. EN 1992-1-1:2004. Eurocode 2: Design of concrete structures Part 1-1: General rules and rules for buildings. Standard, December 2004.
- [111] Fairhurst, C. E. and Hudson, J. Draft ISRM suggested method for the complete stress-strain curve for intact rock in uniaxial compression. *International Journal of Rock Mechanics and Mining Sciences & Geomechanics Abstracts*, 36:279–289, 1999.
- [112] Farmer, I. W. Stress distribution along a resin grouted rock anchor. *International Journal of Rock Mechanics and Mining Sciences & Geomechanics Abstracts*, 12(11):347–351, November 1975.
- [113] Farmer, I. W. Engineering Behaviour of Rocks. Springer Netherlands, 1st edition, 1983.
- [114] Fasching, F. and Vanek, R. Engineering geological characterisation of fault rocks and fault zones. *Geomechanics and Tunnelling*, 4(3):181–194, June 2011.
- [115] Faulkner, D. R., Lewis, A. C., and Rutter, E. H. On the internal structure and mechanics of large strike-slip fault zones: field observations of the Carboneras fault in southeastern Spain. *Tectonophysics*, 367(3-4):235–251, June 2003.
- [116] Faulkner, D. R., Jackson, C. A. L., Lunn, R. J., Schlische, R. W., Shipton, Z. K., Wibberley, C. A. J., and Withjack, M. O. A review of recent developments concerning the structure, mechanics and fluid flow properties of fault zones. *Journal of Structural Geology*, 32(11): 1557–1575, November 2010.
- [117] Feder, G. and Arwanitakis, M. Zur Gebirgsmechanik ausbruchsnaher Bereiche tiefliegender Hohlraumbauten (unter zentralsymmetrischer Belastung). Berg- und Hüttenmännische Monatshefte, 121(4):103–117, 1976.

BIBLIOGRAPHY 295 of 498

[118] Feenstra, P. H. and de Borst, R. Aspects of Robust Computational Models for Plain and Reinforced Concrete. *HERON*, 38(4):1–76, 1993.

- [119] Feynman, R. P., Leighton, R. B., and Sands, M. The Feynman Lectures on Physics, volume I: Mainly Mechanics, Radiation, and Heat. Basic Books, 2010.
- [120] fib. Structural Concrete: Textbook on Behaviour, Design and Performance: Updated knowledge of the CEB/FIP Model Code 1990. Technical report, fédération internationale du béton (fib), Lausanne, Switzerland, July 2000.
- [121] fib. CEB-FIP Model Code for Concrete Structures 2010. Technical report, fédération internationale du béton (fib), 2013.
- [122] Fischnaller, G. Untersuchungen zum Verformungsverhalten von jungem Spritzbeton im Tunnelbau—Grundlagen und Versuche. Master's thesis, University of Innsbruck, Innsbruck, Austria, 1992.
- [123] Fjellström, P. Measurement and Modelling of Young Concrete Properties. Licentiate thesis, Luleå University of Technology, Luleå, Sweden, 2013.
- [124] Forth, J. P. Predicting the tensile creep of concrete. Cement and Concrete Composites, 55: 70–80, January 2015.
- [125] Fossen, H. Structural Geology. Cambridge University Press, 2nd edition, 2016.
- [126] GEOKON. Instruction Manual: Model 4200 Series, Vibrating Wire Strain Gauges. Version: 11/08/2019 (revision DD). Technical report, Lebanon, New Hampshire, USA, 2019.
- [127] Glawe, U. and Upreti, B. N. Better Understanding the Strengths of Serpentinite Bimrock and Homogeneous Serpentinite. *Felsbau*, 22(5):53–60, 2004.
- [128] Golser, J., Schubert, P., and Rabensteiner, K. A new concept for evaluation of loading in shotcrete linings. In *Proceedings of the International Congress on Progress and Innovation* in *Tunnelling*, volume I, pages 79–85, Toronto, Canada, September 1989.
- [129] Golser, J., Rabensteiner, K., Sigl, O., Aldrian, W., Wedenig, H., Brandl, J., and Maier, C. Materialgesetz für Spritzbeton. Technical report, Bundesministerium für wirtschaftliche Angelegenheiten: Straßenforschung, 1990.
- [130] Goodman, R. E. Introduction to Rock Mechanics. John Wiley & Sons, 2nd edition, 1989.
- [131] Goodman, R. E. Engineering geology: rock in engineering construction. John Wiley & Sons, Inc., 1993.
- [132] Goricki, A. and Pimentel, E. Triaxial Tests on Cataclasites. Rock Mechanics and Rock Engineering, 48(5):2167–2171, November 2014.
- [133] Granet, I., Alvarado, J. L., and Bluestein, M. Thermodynamics and Heat Power. CRC Press, Boca Raton, USA, 9th edition, 2021.
- [134] Grassl, P. and Jirásek, M. Damage-plastic model for concrete failure. *International Journal of Solids and Structures*, 43(22-23):7166–7196, November 2006.
- [135] Graziani, A., Boldini, D., and Ribacchi, R. Practical Estimate of Deformations and Stress Relief Factors for Deep Tunnels Supported by Shotcrete. *Rock Mechanics and Rock Engineering*, 38(5):345–372, June 2005.

BIBLIOGRAPHY 296 of 498

[136] Green, S. J. and Swanson, S. R. Static constitutive relations for concrete. Technical report AFWL-TR-72-244, Air Force Weapons Laboratory, Kirtland Air Force Base, New Mexico, USA, April 1973.

- [137] Groshong, R. H. j. Low-temperature deformation mechanisms and their interpretation. Geological Society of America Bulletin, 100(9):1329–1360, September 1988.
- [138] Gross, D., Hauger, W., and Wriggers, P. Technische Mechanik 4: Hydromechanik, Elemente der Höheren Mechanik, Numerische Methoden. Springer Berlin Heidelberg, 7th edition, 2009.
- [139] Großauer, K. Tunnelling in Heterogeneous Ground—Numerical Investigation of Stresses and Displacements. Diploma thesis, Graz University of Technology, Graz, Austria, October 2001.
- [140] Großauer, K. Expert System Development for the Evaluation and Interpretation of Displacement Monitoring Data in Tunnelling. PhD thesis, Graz University of Technology, Graz, Austria, February 2009.
- [141] Grübl, P., Weigler, H., and Karl, S. Beton—Arten, Herstellung und Eigenschaften. Ernst & Sohn Verlag, Berlin, 2nd edition, 2001.
- [142] Gruppe TUNNEL:Monitor. TUNNEL:monitor (v2021.1.4). URL https://igt-engineering.com/de/forschung-und-entwicklung/tunnelmonitor/. Last access: 15.11.2022.
- [143] Gschwandtner, G. G. Analytische Berechnungsansätze zum Kennlinienverfahren. Master's thesis, Montanuniversität Leoben, Leoben, Austria, January 2010.
- [144] Gudmundsson, A., Simmenes, T. H., Larsen, B., and Philipp, S. L. Effects of internal structure and local stresses on fracture propagation, deflection, and arrest in fault zones. *Journal of Structural Geology*, 32(11):1643–1655, November 2010.
- [145] Guntli, P., Keller, F., Lucchini, R., and Rust, S. Gotthard-Basistunnel: Geologie, Geotechnik, Hydrologie zusammenfassender Schlussbericht. Technical report 7, Landesgeologie, 2016.
- [146] Guo, P. and Su, X. Shear strength, interparticle locking, and dilatancy of granular materials. Canadian Geotechnical Journal, 44(5):579–591, May 2007.
- [147] Harer, G., Prein, R., Schwab, P., and Wehr, H. Tunnelling in Poor Ground Conditions Case History Galgenbergtunnel. *Felsbau*, 14(2):82–86, 1996.
- [148] Hartog, A. H. An Introduction to Distributed Optical Fibre Sensors. CRC Press, May 2017.
- [149] Hauggaard-Nielsen, A. B. Mathematical Modelling and Experimental Analysis of Early Age Concrete. PhD thesis, Technical University of Denmark, Lyngby, Denmark, October 1997.
- [150] Havlásek, P., Šmilauer, V., Hájková, K., and Baquerizo, L. Thermo-mechanical simulations of early-age concrete cracking with durability predictions. In *IOP Conference Series:*Materials Science and Engineering, volume 236, pages 1–7. IOP Publishing, September 2017.
- [151] Heinisch, M., Mayr, B., Millen, B., and Holzer, R. Semmering Base Tunnel, construction lot SBT 1.1, access tunnel Göstritz—Geotechnical horizontal and longitudinal section. Project document (in german), 2016.

BIBLIOGRAPHY 297 of 498

[152] Heinisch, M., Mayr, B., Millen, B., and Holzer, R. Semmering Base Tunnel, construction lot SBT 1.1, access tunnel Göstritz—Engineering geological documentation. Project document (in german), Austrian Federal Railways, 2016.

- [153] Heinrich, P. J. Effiziente Erfassung viskoelastischer Eigenschaften bei der Spannungsermittlung von gezwängten Betonbauteilen. PhD thesis, Graz University of Technology, Graz, Austria, November 2018.
- [154] Hellmich, C. Shotcrete as part of the New Austrian Tunneling Method: From Thermochemomechanical Material Modeling to Structural Analysis and Safety Assessment of Tunnels. PhD thesis, Vienna University of Technology, Vienna, Austria, 1999.
- [155] Hellmich, C., Ulm, F.-J., and Mang, H. A. Multisurface Chemoplasticity. I: Material Model for Shotcrete. *Journal of Engineering Mechanics*, 125(6):692–701, 1999.
- [156] Hellmich, C., Ulm, F.-J., and Mang, H. A. Multisurface Chemoplasticity. II: Numerical Studies on NATM Tunneling. *Journal of Engineering Mechanics*, 125(6):702–713, 1999.
- [157] Hellmich, C., Sercombe, J., Ulm, F.-J., and Mang, H. A. Modeling of Early-Age Creep of Shotcrete. II: Application to Tunneling. *Journal of Engineering Mechanics*, 126(3):292–299, 2000.
- [158] Hellmich, C., Mang, H. A., and Ulm, F.-J. Hybrid method for quantification of stress states in shotcrete tunnel shells: combination of 3D in situ displacement measurements and thermochemoplastic material law. *Computers & Structures*, 79(22):2103–2115, 2001.
- [159] Henzinger, M. R., Schachinger, T., Lienhart, W., Buchmayer, F., Weilinger, W., Stefaner, R., Haberler-Weber, M., Haller, E.-M., Steiner, M., and Schubert, W. Fibre-optic supported measurement methods for monitoring rock pressure. *Geomechanics and Tunnelling*, 11(3): 251–263, June 2018.
- [160] Hettler, A. and Vardoulakis, I. Behaviour of dry sand tested in a large triaxial apparatus. Géotechnique, 34(2):183–197, June 1984.
- [161] Hill, R. The mathematical theory of plasticity. The Clarendon Press, Oxford, 1951.
- [162] Hodgson, K. and Cook, N. G. W. The effects of size and stress gradient on the strength of rock. In Proceedings of the 2nd Congress of the International Society for Rock Mechanics, volume 2, pages 31–34, Belgrade, Serbia, September 1970.
- [163] Hoek, E. and Brown, E. T. Practical estimates of rock mass strength. *International Journal of Rock Mechanics and Mining Sciences*, 34(8):1165–1186, December 1997.
- [164] Hoek, E. and Diederichs, M. S. Empirical estimation of rock mass modulus. *International Journal of Rock Mechanics and Mining Sciences*, 43(2):203–215, February 2006.
- [165] Hoek, E. Brittle failure of rock. Rock Mechanics in Engineering Practice. Wiley: New York, 1968.
- [166] Hoek, E. and Brown, E. T. *Underground Excavations in Rock*. CRC Press, 1st edition, 1980.
- [167] Hoek, E. and Brown, E. T. Empirical Strength Criterion for Rock Masses. *Journal of the Geotechnical Engineering Division*, 106(9):1013–1035, September 1980.

BIBLIOGRAPHY 298 of 498

[168] Holt, E. E. Early age autogeneous shrinkage of concrete. Vtt publications 446, Technical Research Centre of Finland, Espoo, Finland, 2001.

- [169] Holter, K. G. Properties of waterproof sprayed concrete tunnel linings: A study of EVAbased sprayed membranes for waterproofing of rail and road tunnels in hard rock and cold climate. PhD thesis, Norwegian University of Science and Technology, Trondheim, Norway, December 2015.
- [170] Holzer, R. Personal communication, September 2022.
- [171] Holzer, R., Prall, K., Wagner, O. K., and Gobiet, G. Semmering Base Tunnel Tunnelling in challenging geotechnical and geological conditions in major fault zones. *Geomechanics* and *Tunnelling*, 13(5):509–518, October 2020.
- [172] Hösthagen, A. Thermal Crack Risk Estimation and Material Properties of Young Concrete. Licentiate thesis, Luleå University of Technology, Luleå, Sweden, 2017.
- [173] Huber, H. Untersuchungen zum Verformungsverhalten von jungem Spritzbeton im Tunnelbau. Master's thesis, University of Innsbruck, Innsbruck, Austria, 1991.
- [174] Ikumi, T., Salvador, R. P., and Aguado, A. Mix proportioning of sprayed concrete: A systematic literature review. *Tunnelling and Underground Space Technology*, 124(104456): 12, June 2022.
- [175] Itasca Consultants S.A.S. Dynamic Analysis in FLAC3D. Electronical, 2020. URL https://www.itasca.fr/software/dynamic-analysis-in-flac3d. Last access: 23.12.2020.
- [176] Itasca Consulting Group, Inc. UDEC 5.0 documentation, 2011.
- [177] Itasca Consulting Group, Inc. FLAC3D 6.0 documentation, 2017.
- [178] Itasca Consulting Group, Inc. FLAC3D 7.0 documentation, 2019.
- [179] Itasca Consulting Group, Inc. Learning Itasca Educational Partnership. Electronical, 2023. URL https://www.itascainternational.com/learning/iep/iep-research-program. Last access: 05.01.2023.
- [180] Jaeger, J. C. and Cook, N. G. W. Fundamentals of Rock Mechanics. Chapman & Hall: London, 3rd edition, 1979.
- [181] Jaeger, J. C., Cook, N. G. W., and Zimmerman, R. W. Fundamentals of Rock Mechanics. Blackwell Publishing, 4th edition, 2007.
- [182] Johnson, R. B. and DeGraff, J. V. Principles of Engineering Geology. John Wiley & Sons, Inc., 1988.
- [183] Johnston, I. W. Strength of Intact Geomechanical Materials. *Journal of Geotechnical Engineering*, 111(6):730–749, June 1985.
- [184] Kahraman, S. and Alber, M. Estimating unconfined compressive strength and elastic modulus of a fault breccia mixture of weak blocks and strong matrix. *International Journal of Rock Mechanics and Mining Sciences*, 43(8):1277–1287, December 2006.

BIBLIOGRAPHY 299 of 498

[185] Kahraman, S., Alber, M., Fener, M., and Gunaydin, O. Evaluating the geomechanical properties of Misis fault breccia (Turkey). *International Journal of Rock Mechanics and Mining Sciences*, 45(8):1469–1479, December 2008.

- [186] Kahraman, S., Gunaydin, O., Alber, M., and Fener, M. Evaluating the strength and deformability properties of Misis fault breccia using artificial neural networks. *Expert Systems with Applications*, 36(3):6874–6878, April 2009.
- [187] Kainrath-Reumayer, S., Gschwandtner, G., Schuller, E., and Galler, R. Beitrag zur Anwendung des Kennlinienverfahrens. *Berg- und Hüttenmännische Monatshefte*, 155(2): 83–89, February 2010.
- [188] Kainrath-Reumayer, S., Neugebauer, E., Charette, F., Plouffe, M., and Galler, R. Ankerung im Untertagebau - Entwicklungen in Theorie und Praxis. Geomechanik und Tunnelbau, 1 (5):345–351, October 2008.
- [189] Kaiser, P. K. and Kim, B. H. Rock mechanics challenges of underground constructions and mining. In *Proceedings of the Korean Rock Mechanics Symposium*, pages 1–16, Seoul, South Korea, 2008. Korean Society for Rock Mechanics.
- [190] Kaiser, P. K. and Tannant, D. D. The Role of Shotcrete in Hard Rock Mines. In Hustrulid, W. A. and Bullock, R. L., editors, *Underground Mining Methods—Engineering Fundamentals* and International Case Studies, chapter 67, pages 579–592. Society for Mining, Metallurgy, and Exploration, Inc. (SME), 2001.
- [191] Kaiser, P. K., Diederichs, M. S., Martin, C. D., Sharp, J., and Steiner, W. Underground Works In Hard Rock Tunnelling And Mining. In *Proceedings of the International Conference on Geotechnical & Geological Engineering (GeoEng2000)*, ISRM International Symposium, pages 841–926, Melbourne, Australia, November 2000. Technomic Publishing Co.
- [192] Kaiser, P. K., Amann, F., and Steiner, W. How Highly Stressed Brittle Rock Failure Impacts Tunnel Design. In Proceedings of the 2010 Regional Symposium of the International Society for Rock Mechanics (EUROCK 2010), pages 1–12, Lausanne, Switzerland, June 2010. ISRM-EUROCK-2010-003.
- [193] Kalender, A., Sönmez, H., Medley, E. W., Tunusluoglu, C., and Kasapoglu, K. E. An approach to predicting the overall strengths of unwelded bimrocks and bimsoils. *Engineering Geology*, 183:65–79, December 2014.
- [194] Kastner, H. Statik des Tunnel- und Stollenbaues: auf der Grundlage geomechanischer Erkenntnisse. Springer Berlin Heidelberg, 1962.
- [195] Kettunen Linder, M. and Kilic, O. En studie av sprutbetongförstärkningen i Citybanan -Norrströmstunneln. Master's thesis, KTH Royal Insitute of Technology, Stockholm, Sweden, March 2011. Examensarbete 326.
- [196] Kim, Y.-S., Peacock, D. C. P., and Sanderson, D. J. Fault damage zones. *Journal of Structural Geology*, 26(3):503–517, March 2004.
- [197] Kirsch, G. Die Theorie der Elastizität und die Bedürfnisse der Festigkeitslehre. Zeitschrift des Vereines Deutscher Ingenieure, 42(29):797–807, 1898.

BIBLIOGRAPHY 300 of 498

[198] Klein, C. and Philpotts, A. R. Earth materials: introduction to mineralogy and petrology. Cambridge University Press, 1st edition, 2013.

- [199] Kluckner, A. Aspekte der Gebirgscharakterisierung im Tunnelbau. Master's thesis, Graz University of Technology, Graz, Austria, October 2012.
- [200] Kluckner, A. and Schubert, W. Study on the Anisotropic Displacement Pattern at a Conventional Tunnel Drive. In *Proceedings of the 5th ISRM Young Scholars' Symposium on Rock Mechanics and International Symposiumon Rock Engineering for Innovative Future (YSRM2019 & REIF2019)*, pages 1–6, Okinawa, Japan, December 2019.
- [201] Knipe, R. J. Deformation mechanism path diagrams for sediments undergoing lithification. Structural Fabric in Deep Sea Drilling Project Cores From Forearcs, Memoir 166:151–160, 1986.
- [202] Kovler, K. Why sealed concrete swells. ACI Materials Journal, 93(4):334-340, 1996.
- [203] Kropik, C. and Mang, H. A. Computational mechanics of the excavation of tunnels. Engineering Computations, 13(7):49–69, November 1996.
- [204] Kulhawy, F. H. Stress deformation properties of rock and rock discontinuities. *Engineering Geology*, 9(4):327–350, December 1975.
- [205] Kusterle, W. Qualitätsverbesserungen beim Spritzbeton durch technologische Massnahmen, durch den Einsatz neuer Materialien und auf Grund der Erfassung von Spritzbetoneigenschaften. Habilitation dissertation, University of Innsbruck, Innsbruck, Austria, 1992.
- [206] Kusterle, W. Comparison of shrinkage behaviour and creep properties under different compressive stress levels for wet-mix sprayed concrete from ten hours up to two weeks. Technical report, Morgan Tunnelling, 1999.
- [207] Kusterle, W. and Lukas, W. Spritzbeton hoher Güte für die einschalige Spritzbetonbauweise. In Tagungsband der 3. Internationalen Fachtagung Spritzbeton-Technologie, Innsbruck, Austria, pages 29–40, 1990.
- [208] Kusterle, W., Jäger, J., John, M., Neumann, C., and Röck, R. Spritzbeton im Tunnelbau. In Bergmeister, K., Fingerloos, F., and Wörner, J.-D., editors, Beton-Kalender 2014: Unterirdisches Bauen, Grundbau, Eurocode 7, chapter IX, pages 303–390. Ernst & Sohn GmbH & Co. KG., 2014.
- [209] Kuwajima, F. M. Early Age Properties of Shotcrete. In Celestino, T. B. and Parker, H. W., editors, Proceedings of the Eighth International Conference on Shotcrete for Underground Support, São Paulo, Brazil, April 1999. American Society of Civil Engineers.
- [210] Lackner, R. and Mang, H. A. Cracking in shotcrete tunnel shells. *Engineering Fracture Mechanics*, 70(7–8):1047–1068, May 2003.
- [211] Lackner, R., Hellmich, C., and Mang, H. A. Constitutive modeling of cementitious materials in the framework of chemoplasticity. *International Journal for Numerical Methods in Engineering*, 53(10):2357–2388, 2002.
- [212] Lackner, R., Macht, J., Hellmich, C., and Mang, H. A. Hybrid Method for Analysis of Segmented Shotcrete Tunnel Linings. *Journal of Geotechnical and Geoenvironmental Engineering*, 128(4):298–308, April 2002.

BIBLIOGRAPHY 301 of 498

[213] Lama, R. D. and Vutukuri, V. S. *Handbook on Mechanical Properties of Rocks*, volume 2 of *Series on Rock and Soil Mechanics*. Trans Tech Publications, Clausthal, Germany, 1978.

- [214] Laplante, P. Propriétés mécaniques des bétons durcissants: analyse comparée des bétons classiques et à très hautes performances [Mechanical properties of hardening concrete: a comparative analysis of classical and high strength concretes]. PhD thesis, Ecole Nationale des Ponts et Chaussées, Paris, France, 1993.
- [215] Laplante, P. and Boulay, C. Evolution du coefficient de dilatation thermique du béton en fonction de sa maturité aux tout premiers âges. *Materials and Structures*, 27(10):596–605, December 1994.
- [216] Leber, C. Einfluss der Primärspannungsorientierung auf die Verschiebungscharakteristik. Master's thesis, Graz University of Technology, Graz, Austria, March 2009.
- [217] Lebschy, D. Investigation of the influence of the tunnel lining on the displacement development. Master's thesis, Graz University of Technology, Graz, Austria, September 2014.
- [218] Lenz, G. Displacement monitoring data in tunnelling—Development of a semiautomatic evaluation system. Diploma thesis, Graz University of Technology, Graz, Austria, April 2007.
- [219] Lenz, G. Characterization of ground and system behaviour in water-bearing fault zones. PhD thesis, Graz University of Technology, Graz, Austria, July 2020.
- [220] Lenz, G. Personal communication, May 2022.
- [221] Lenz, G. Personal communication, July 2022.
- [222] Lenz, G. Personal communication, November 2022.
- [223] Lepique, M. Empfehlung Nr. 10 des Arbeitskreises 3.3 "Versuchstechnik Fels" der Deutschen Gesellschaft für Geotechnik e. V.: Indirekter Zugversuch an Gesteinsproben Spaltzugversuch. Bautechnik, 85(9):623–627, September 2008.
- [224] Lienhart, W., Schubert, W., Henzinger, M. R., Buchmayer, F., Weilinger, W., and Stefaner, R. Faseroptisch unterstützte Messmethoden zur Beobachtung von Gebirgsdruck. Research report, Federal Ministry Republic of Austria, Climate Action, Environment, Energy, Mobility, Innovation and Technology, Vienna, Austria, October 2018.
- [225] Lindlar, B., Jahn, M., and Schlumpf, J. Sika Sprayed Concrete Handbook. Sika AG, 2020. URL https://www.sika.com/content/dam/dms/corporate/n/glo-sprayed-concrete-handbook-2021.pdf. Last access: 14.01.2023.
- [226] Lindquist, E. S. and Goodman, R. E. Strength and deformation properties of a physical model melange. In Nelson, P. P. and Laubach, S. E., editors, Rock Mechanics - Models and Measurements - Challenges from Industry: Proceedings of the 1st North American Rock Mechanics Symposium (NARMS), pages 843–850. The University of Texas at Austin, A.A. Balkema: Rotterdam, June 1994.
- [227] Lindquist, E. S. The Strength and Deformation Properties of Melange. PhD thesis, University of California, Berkeley, California, USA, 1994.

BIBLIOGRAPHY 302 of 498

[228] Lockner, D. A. Rock Physics and Phase Relations: A Handbook of Physical Constants, volume 3 of AGU Reference Shelf, chapter Rock Failure, pages 127–147. American Geophysical Union, Washington, D.C., USA, 1st edition, January 1995.

- [229] Logan, J. M., Friedmann, M., Higgs, N., Dengo, C., and Shimamoto, T. Experimental studies of simulated gouge and their application to studies of natural fault zones. In Proceedings of Conference VIII—Analysis of Actual Fault Zones in Bedrock, pages 305—343, Menlo Park, California, USA, April 1979. United States Department of the Interior, Geological Survey, Office of Earthquake Studies. Open-file report 79-1239.
- [230] Lu, T. Autogenous shrinkage of early age cement paste and mortar. PhD thesis, Delft University of Technology, Delft, Netherlands, 2019.
- [231] Lucarelli, A. Personal communication, June 2022.
- [232] Luna Innovations Inc. Datasheet: Luna Optical Backscatter Reflectometer (OBR) Model 4600. Version: LTOBR4600 REV. 004 02/13/2014. Technical report, Blacksburg, Virginia, USA, 2014.
- [233] Luna Innovations Inc. Datasheet: Luna Optical Backscatter Reflectometer (OBR) Model 4600. Version: LTOBR4600 REV. 006 03/09/2018. Technical report, Blacksburg, Virginia, USA, 2018.
- [234] Lupini, J. F., Skinner, A. E., and Vaughan, P. R. The drained residual strength of cohesive soils. *Géotechnique*, 31(2):181–213, June 1981.
- [235] Ma, J. Faserfreier Ultrahochfester Beton—Entwicklung und Materialeigenschaften. PhD thesis, Leipzig University, Leipzig, Germany, 2010.
- [236] Macht, J. Hybrid Analysis of Shotcrete Tunnel Linings: Assessment and Online Monitoring of the Level of Loading. PhD thesis, Vienna University of Technology, Vienna, Austria, 2002.
- [237] Mair, K., Frye, K. M., and Marone, C. Influence of grain characteristics on the friction of granular shear zones. *Journal of Geophysical Research: Solid Earth*, 107(B10):ECV 4–1–ECV 4–9, October 2002.
- [238] Małkowski, P., Ostrowski, L., and Brodny, J. Analysis of Young's modulus for Carboniferous sedimentary rocks and its relationship with uniaxial compressive strength using different methods of modulus determination. *Journal of Sustainable Mining*, 17(3):145–157, 2018.
- [239] Mandl, G. Discontinuous fault zones. *Journal of Structural Geology*, 9(1):105–110, January 1987.
- [240] Mandl, G. Mechanics of Tectonic Faulting: Models and Basic Concepts. Developments in Structural Geology, 1. Elsevier Science Publishers B.V.: Amsterdam, 1988.
- [241] Mandl, G. Faulting in Brittle Rocks: An Introduction to the Mechanics of Tectonic Faults. Springer Berlin Heidelberg, 1st edition, 2000.
- [242] Mang, H. A. and Hofstetter, G. Festigkeitslehre. Springer Berlin Heidelberg, 5th edition, 2018.

BIBLIOGRAPHY 303 of 498

[243] Manton, N. and Mee, N. *The Physical World*. Oxford University Press, 1st edition, April 2017.

- [244] Marcher, T. Personal communication, January 2021.
- [245] Marinos, P. V. and Tsiambaos, G. Strength and Deformability of Specific Sedimentary and Ophiolithic Rocks. *Bulletin of the Geological Society of Greece*, 43(3):1259–1266, January 2010.
- [246] Marshak, S. Earth: portrait of a planet. New York: W.W. Norton & Company, 6th edition, 2019.
- [247] Martin, J. Back-analysis of rock mass parameters at the Semmering Base Tunnel based on the convergence confinement method. Master's thesis, Graz University of Technology, Graz, Austria, December 2022.
- [248] Medley, E. W. Using stereological methods to estimate the volumetric proportions of blocks in melanges and similar block-in-matrix rocks (bimrocks). In Oliveira, R., Rodrigues, L. F., Coelho, A. G., and Cunha, A. P., editors, *Proceedings of the 7th International Congress of the International Association of Engineering Geology (IAEG)*, pages 1031–1040. A.A. Balkema: Rotterdam, September 1994.
- [249] Medley, E. W. Systematic Characterization of Melange Bimrocks and Other Chaotic Soil/Rock Mixtures. Felsbau, 17(3):152–162, 1999.
- [250] Medley, E. W. Orderly Characterization of Chaotic Franciscan Melanges. *Felsbau*, 19(4): 20–33, 2001.
- [251] Medley, E. W. Observations on Tortuous Failure Surfaces in Bimrocks. *Felsbau*, 22(5): 35–43, 2004.
- [252] Medley, E. Tunneling Through Fault Zones and Melanges. Lecture slides of lecture 4 of the short course "Anticipating and addressing the characterization, design and construction problems of fault rocks, melanges and other bimrocks", Geological Engineering Department, Hacettepe University, Ankara, Turkey, June 2004.
- [253] Medley, E. W. Estimating Block Size Distributions of Melanges and Similar Block-in-Matrix Rocks (Bimrocks). In Hammah, R., Bawden, W., Curran, J., and Telesnicki, M., editors, Proceedings of 5th North American Rock Mechanics Symposium (NARMS), pages 599–606, Toronto, Canada, July 2002. University of Toronto Press.
- [254] Medley, E. W. and Zekkos, D. Geopractitioner approaches to working with antisocial mélanges. In Mélanges: Processes of Formation and Societal Significance, number 480, pages 261–277. The Geological Society of America, 2011.
- [255] Medley, E. W. The Engineering Characterization of Melanges and Similar Block-in-Matrix Rocks (Bimrocks). PhD thesis, University of California, Berkeley, California, USA, 1994.
- [256] Medley, E. W. and Lindquist, E. S. The engineering significance of the scale-independence of some Franciscan melanges in California, USA. In Daemen, J. J. K. and Schultz, R. A., editors, *Proceedings of the 35th U.S. Symposium on Rock Mechanics*, pages 907–914. A.A. Balkema, Rotterdam, 1995.

BIBLIOGRAPHY 304 of 498

[257] Meixner, T. Trigger Values for tunnel monitoring in SCL shallow tunnels. Master's thesis, Graz University of Technology, Graz, Austria, September 2016.

- [258] Menétrey, P. and Willam, K. J. Triaxial Failure Criterion for Concrete and its Generalization. ACI Structural Journal, 92(3):311–318, 1995.
- [259] Merriam-Webster, Inc. Dictionary: Autogenous. Electronical, 2020. URL https://www.merriam-webster.com/dictionary/autogenous. Last access: 23.06.2020.
- [260] Meschke, G. Consideration of aging of shotcrete in the context of a 3-D viscoplastic material model. *International Journal for Numerical Methods in Engineering*, 39:3123–3143, 1996.
- [261] Meschke, G., Kropik, C., and Mang, H. A. Numerical analyses of tunnel linings by means of a viscoplastic material model for shotcrete. *International Journal for Numerical Methods* in Engineering, 39:3145–3162, 1996.
- [262] Michelis, P. N. Work-softening and hardening behaviour of granular rocks. *Rock Mechanics*, 14(3):187–200, December 1981.
- [263] Mindess, S., Young, J. F., and Lawrence, F. V. Creep and drying shrinkage of calcium silicate pastes I. Specimen preparation and mechanical properties. *Cement and Concrete Research*, 8(5):591–600, 1978.
- [264] Mitchell, T. M. and Faulkner, D. R. The nature and origin of off-fault damage surrounding strike-slip fault zones with a wide range of displacements: A field study from the Atacama fault system, northern Chile. *Journal of Structural Geology*, 31(8):802–816, August 2009.
- [265] Mödlhammer, H. *Spritzbeton: In situ Versuche*. Bachelor's thesis, Montanuniversität Leoben, Leoben, Austria, April 2008.
- [266] Monsberger, C. M., Lienhart, W., Kluckner, A., Wagner, L., and Schubert, W. Continuous strain measurements in a shotcrete tunnel lining using distributed fibre optic sensing. In *Proceedings of the 9th European Workshop on Structural Health Monitoring*, pages 1–13, Manchester, United Kingdom, July 2018.
- [267] Monsberger, C. M., Lienhart, W., Kluckner, A., and Schubert, W. In-situ assessment of distributed strain and curvature characteristics in shotcrete tunnel linings based on fiber optic strain sensing. In *Proceedings of the 14th International Congress on Rock Mechanics* and Rock Engineering, pages 1–8, Foz do Iguassu, Brazil, September 2019.
- [268] Monsberger, C. M. and Lienhart, W. Distributed fiber optic shape sensing along shotcrete tunnel linings: Methodology, field applications, and monitoring results. *Journal of Civil Structural Health Monitoring*, 11(2):337–350, January 2021.
- [269] Monsberger, C. M., Bauer, P., Buchmayer, F., and Lienhart, W. Large-scale distributed fiber optic sensing network for short and long-term integrity monitoring of tunnel linings. *Journal of Civil Structural Health Monitoring*, 12(6):1317–1327, March 2022.
- [270] Moritz, B., Grossauer, K., and Schubert, W. Short Term Prediction of System Behaviour of Shallow Tunnels in Heterogeneous Ground. *Felsbau*, 22(5):44–52, 2004.
- [271] Müller, M. Kriechversuche an jungen Spritzbetonen zur Ermittlung der Parameter für Materialgesetze. mathesis, Montanuniversität Leoben, Leoben, Austria, October 2001.

BIBLIOGRAPHY 305 of 498

[272] Mutschler, T. Neufassung der Empfehlung Nr. 1 des Arbeitskreises "Versuchstechnik Fels" der Deutschen Gesellschaft für Geotechnik e. V.: Einaxiale Druckversuche an zylindrischen Gesteinsprüfkörpern. *Bautechnik*, 81(10):825–834, October 2004.

- [273] Naylor, M. A., Mandl, G., and Supesteijn, C. H. K. Fault geometries in basement-induced wrench faulting under different initial stress states. *Journal of Structural Geology*, 8(7): 737–752, January 1986.
- [274] Nefeslioglu, H. A. Evaluation of geo-mechanical properties of very weak and weak rock materials by using non-destructive techniques: Ultrasonic pulse velocity measurements and reflectance spectroscopy. *Engineering Geology*, 160:8–20, June 2013.
- [275] Neuner, M., Cordes, T., Drexel, M., and Hofstetter, G. Time-Dependent Material Properties of Shotcrete: Experimental and Numerical Study. *Materials*, 10(9):1067, September 2017.
- [276] Neuner, M., Gamnitzer, P., and Hofstetter, G. An Extended Damage Plasticity Model for Shotcrete: Formulation and Comparison with Other Shotcrete Models. *Materials*, 10(1): 1–22, January 2017.
- [277] Neuner, M., Schreter, M., Unteregger, D., and Hofstetter, G. Influence of the Constitutive Model for Shotcrete on the Predicted Structural Behavior of the Shotcrete Shell of a Deep Tunnel. *Materials*, 10(6):1–17, May 2017.
- [278] Neuner, M., Gamnitzer, P., and Hofstetter, G. Correction: An Extended Damage Plasticity Model for Shotcrete: Formulation and Comparison with Other Shotcrete Models. *Materials*, 11(1):135, January 2018.
- [279] Neville, A. M. Properties of Concrete. Prentice Hall, 4th edition, 1995.
- [280] Neville, A. M., Dilger, W. H., and Brooks, J. J. Creep of plain and structural concrete. Construction Press (Longman), Harlow, UK, 1983.
- [281] Nielsen, L. F. Composite creep analysis of concrete: A rational, incremental stress-strain approach. Byg Rapport R-178, Technical University of Denmark, Lyngby, Denmark, 2007.
- [282] Nilsson, M. Restraint Forces and Partial Coefficients for Crack Risk Analyses of Early Age Concrete Structures. PhD thesis, Luleå University of Technology, Luleå, Sweden, 2003.
- [283] Nübel, K. and Huang, W. A study of localized deformation pattern in granular media. Computer Methods in Applied Mechanics and Engineering, 193(27-29):2719–2743, July 2004.
- [284] Oberdörfer, W. Auswirkung von unterschiedlichen Betonnachbehandlungsmassnahmen auf die Qualit\u00e4t des Nassspritzbetons. Master's thesis, University of Innsbruck, Innsbruck, Austria, 1996.
- [285] Obert, L. and Duvall, W. I. Rock Mechanics and the Design of Structures in Rock. John Wiley & Sons, New York, 1967.
- [286] Obert, L., Windes, S. L., and Duvall, W. I. Standardized tests for determining the physical properties of mine rock. Report of Investigations 3891, United States Department of the Interior-Bureau of Mines, August 1946.

BIBLIOGRAPHY 306 of 498

[287] Obrzud, R. F. and Truty, A. The Hardening Soil Model-A practical guidebook (Z\_Soil.PC 100701 report, revised 21.10.2018). Zace Services Ltd, October 2018.

- [288] ÖBV. Spritzbeton: Teil 1—Anwendung. Guideline, Österreichischer Betonverein (ÖBV), 1989.
- [289] ÖBV. Sprayed Concrete. Guideline, Österreichische Bautechnik Vereinigung (ÖBV), April 2013.
- [290] ÖGG. Guideline for the Geotechnical Design of Underground Structures with Conventional Excavation. Guideline, Austrian Society for Geomechanics (ÖGG), Salzburg, Austria, 2010. Translated from German version 2.1.
- [291] ÖGG. Geotechnical Monitoring in Conventional Tunnelling. Austrian Society for Geomechanics (ÖGG), Salzburg, Austria, 2014.
- [292] Oluokun, F. A., Burdette, E. G., and Deatherage, J. H. Splitting Tensile Strength and Compressive Strength Relationships at Early Ages. ACI Materials Journal, 88(2):115–121, 1991.
- [293] Ord, A. Deformation of rock: A pressure-sensitive, dilatant material. *Pure and Applied Geophysics (PAGEOPH)*, 137(4):337–366, 1991.
- [294] Oreste, P. P. A Procedure for Determining the Reaction Curve of Shotcrete Lining Considering Transient Conditions. Rock Mechanics and Rock Engineering, 36(3):209–236, June 2003.
- [295] Oreste, P., Spagnoli, G., and Ceravolo, L. A. A numerical model to assess the creep of shotcrete linings. Proceedings of the Institution of Civil Engineers - Geotechnical Engineering, 172(4):344–354, August 2019.
- [296] Palkovic, S. D., Brommer, D. B., Kupwade-Patil, K., Masic, A., Buehler, M. J., and
   Büyüköztürk, O. Roadmap across the mesoscale for durable and sustainable cement paste
   A bioinspired approach. Construction and Building Materials, 115:13-31, July 2016.
- [297] Palmström, A. and Singh, R. The deformation modulus of rock masses comparisons between in situ tests and indirect estimates. *Tunnelling and Underground Space Technology*, 16(2):115–131, April 2001.
- [298] Parent, T., Domede, N., Sellier, A., and Mouatt, L. Mechanical characterization of limestone from sound velocity measurement. *International Journal of Rock Mechanics and Mining* Sciences, 79:149–156, October 2015.
- [299] Passchier, C. W. and Trouw, R. A. J. Microtectonics. Springer Verlag, Berlin, 1996.
- [300] Paulini, P. Reaction mechanisms of concrete admixtures. Cement and Concrete Research, 20(6):910–918, November 1990.
- [301] Peacock, D. C. P., Dimmen, V., Rotevatn, A., and Sanderson, D. J. A broader classification of damage zones. *Journal of Structural Geology*, 102:179–192, 2017.
- [302] Pichler, B. and Hellmich, C. Hybrid methods for shotcrete and segmental linings tunnel shells Combining displacement and rotation measurements with computational multiscale mechanics. *Geomechanics and Tunnelling*, 11(3):226–235, June 2018.

BIBLIOGRAPHY 307 of 498

[303] Pichler, B., Hellmich, C., and Eberhardsteiner, J. Spherical and acicular representation of hydrates in a micromechanical model for cement paste: prediction of early-age elasticity and strength. *Acta Mechanica*, 203(3-4):137–162, June 2008.

- [304] Pichler, B., Hellmich, C., and Eberhardsteiner, J. Reaktionskinetik und Kriecheigenschaften des Spritzbetons, der im Zuge des Vortriebs des Koralmtunnels (Baulos KAT2) verwendet wird. Technical report (preliminary), Institute for Mechanics of Materials and Struttures, Vienna University of Technology, Vienna, Austria, December 2011.
- [305] Pilgerstorfer, T. Prediction of displacement development using closed form solutions. Diploma thesis, Graz University of Technology, Graz, Austria, May 2008.
- [306] Pilgerstorfer, T. Mechanical Characterization of Fault Zones. PhD thesis, Graz University of Technology, Graz, Austria, 2014.
- [307] Pilgerstorfer, T. Personal communication, January 2022.
- [308] Pilgerstorfer, T., Radončić, N., Moritz, B., and Goricki, A. Evaluation and interpretation of monitoring data in the test adit EKT Paierdorf. Geomechanics and Tunnelling, 4(5): 423–434, October 2011.
- [309] Pittino, G., Galler, R., Bonin, K., and Bezler, J. Experiences with polymer-modified shotcrete. In Amberg, F. and Knut, F. G., editors, *Proceedings of the 11th Conference on Shotcrete for Underground Support*, pages 1–18, Davos, Switzerland, June 2009. Engineering Conferences International (ECI).
- [310] Pötsch, M. The analysis of rotational and sliding modes of failure for slopes, foundations, and underground structures in blocky, hard rock. PhD thesis, Graz University of Technology, Graz, Austria, March 2011.
- [311] Potts, D. M. and Zdravković, L. Finite element analysis in geotechnical engineering: theory. Thomas Telford Ltd, London, 1999.
- [312] Poturovic, S., Schubert, W., and Blümel, M. Comparison of Constant Normal Load (CNL) and Constant Normal Stiffness (CNS) Direct Shear Tests. In Schubert, W. and Kluckner, A., editors, *Proceedings of the ISRM Regional Symposium EUROCK 2015 & 64<sup>th</sup> Geomechanics Colloquium—Future Development of Rock Mechanics*, pages 1–6, Salzburg, Austria, October 2015. Austrian Society for Geomechanics.
- [313] Powers, T. C. Causes and Control of Volume Change. *Journal of the PCA Research and Development Laboratories*, pages 30–39, January 1959. Portland Cement Association (PCA).
- [314] Powers, T. C. and Brownyard, T. L. Studies of the Physical Properties of Hardened Portland Cement Paste. In *Bulletin No. 22*, pages 1–342. Portland Cement Association (PCA), March 1948.
- [315] Probst, B. Entwicklung einer Langzeitdruckversuchsanlage für den Baustellenbetrieb zur Bestimmung des Materialverhaltens von jungem Spritzbeton. Diploma thesis, Montanuniversität Leoben, Leoben, Austria, 1999.
- [316] Pusch, R. Alteration of the Hydraulic Conductivity of Rock by Tunnel Excavation.

  International Journal of Rock Mechanics and Mining Sciences & Geomechanics Abstracts,
  26(1):79–83, January 1989.

BIBLIOGRAPHY 308 of 498

[317] Püstow, H. Tunnelling in a tectonic melange of high structural complexity. mathesis, Aachen University of Technology, Aachen, Germany, 2001.

- [318] R Core Team. R: A Language and Environment for Statistical Computing. R Foundation for Statistical Computing, Vienna, Austria, 2022. URL https://www.R-project.org/. Last access: 14.01.2023.
- [319] Radončić, N. Tunnel design and prediction of systembehaviour in weak ground. PhD thesis, Graz University of Technology, Graz, Austria, March 2011.
- [320] Rastrup, E. Heat of hydration in concrete. *Magazine of Concrete Research*, 6(17):79–92, September 1954.
- [321] Raymond, L. A. Classification of melanges. In Raymond, L. A., editor, *Melanges: Their Nature, Origin, and Significance*, pages 7–20. The Geological Society of America, 1984.
- [322] Reyes, O. and Einstein, H. H. Failure Mechanisms of Fractured Rock—A Fracture Coalescence Model. In Wittke, W., editor, *Proceedings of the 7th International ISRM Congress*, pages 333–339, Aachen, Germany, September 1991. A.A. Balkema.
- [323] Riedmüller, G. and Schubert, W. Tunnelling in Fault Zones Innovative Approaches. In Proceedings of the 4th North American Rock Mechanics Symposium (NARMS 2000): Rock Around The Rim, pages 1–12, Seattle, Washington, USA, July 2000. Balkema: Rotterdam. ARMA-2000-0113.
- [324] Riedmüller, G., Brosch, F. J., Klima, K., and Medley, E. W. Engineering Geological Characterization of Brittle Faults and Classification of Fault Rocks. *Felsbau*, 19(4):13–19, 2001.
- [325] Rokahr, R. B. and Lux, K. H. Einfluß des rheologischen Verhaltens des Spritzbetons auf den Ausbauwiderstand. *Felsbau*, 5(1):11–18, 1987.
- [326] Rombach, G. Spannbetonbau. Wiley-VCH Verlag GmbH, April 2010.
- [327] Roscoe, K. H. The Influence of Strains in Soil Mechanics. *Géotechnique*, 20(2):129–170, June 1970.
- [328] Rosso, R. S. A comparison of joint stiffness measurements in direct shear, triaxial compression, and In Situ. *International Journal of Rock Mechanics and Mining Sciences & Geomechanics Abstracts*, 13(6):167–172, June 1976.
- [329] Rostami, J., Kahraman, S., Yu, X., Copur, H., Balci, C., Bamford, W., and Asbury, B. The relation between uniaxial compressive and Brazilian tensile strength. In Ulusay, R., Aydan, O., Gercek, H., and Hindistan, M. A., editors, Proceedings of the 2016 Regional Symposium of the International Society for Rock Mechanics (EUROCK 2016)—Rock Mechanics and Rock Engineering: From the Past to the Future, volume 1, pages 147–152, Ürgüp, Cappadocia Region, Turkey, August 2016. Turkish National Society for Rock Mechanics, CRC Press.
- [330] Rowe, P. W. The stress-dilatancy relation for static equilibrium of an assembly of particles in contact. *Proceedings of the Royal Society of London. Series A. Mathematical and Physical Sciences*, 269(1339):500–527, October 1962.
- [331] Rowe, R. K., editor. Geotechnical and geoenvironmental engineering handbook. Springer US, 2001.

BIBLIOGRAPHY 309 of 498

[332] Ruetz, W. Das Kriechen des Zementsteins im Beton und seine Beeinflussung durch gleichzeitiges Schwinden. In *Deutscher Ausschuss für Stahlbeton*, number 183. Wilhelm Ernst & Sohn, Berlin, 1966.

- [333] Rust, W. Nichtlineare Finite-Elemente-Berechnungen. Springer Fachmedien Wiesbaden, 3rd edition, 2016.
- [334] Sadd, M. Elasticity. Academic Press, 3rd edition, 2014.
- [335] Sainsbury, B. L. and Sainsbury, D. P. Practical Use of the Ubiquitous-Joint Constitutive Model for the Simulation of Anisotropic Rock Masses. Rock Mechanics and Rock Engineering, 50(6):1507–1528, February 2017.
- [336] Salamon, M. D. G. Energy considerations in rock mechanics: fundamental results. *Journal of the South African Institute of Mining and Metallurgy*, 84:233–246, 1984.
- [337] Saldivar, G. G. and Sánchez, F. A. Tunnels and Underground Cities: Engineering and Innovation meet Archaeology, Architecture and Art, chapter Comparative study on shotcrete performance in tunnels based on different constitutive approaches, pages 1–10. CRC Press, 1st edition, April 2019.
- [338] Sammis, C. G. and Biegel, R. L. Fractals, fault-gouge, and friction. *Pure and Applied Geophysics PAGEOPH*, 131(1-2):255–271, 1989.
- [339] Sausgruber, T. and Brandner, R. The Relevance of Brittle Fault Zones in Tunnel Construction—Lower Inn Valley Feeder Line North of the Brenner Base Tunnel, Tyrol, Austria. *Mitteilungen der Österreichischen Geologischen Gesellschaft*, 94:157–172, August 2003.
- [340] Saw, H. A., Villaescusa, E., Windsor, C. R., and Thompson, A. G. Non-linear, elastic-plastic response of steel fibre reinforced shotcrete to uniaxial and triaxial compression testing. In Amberg, F. and Garshol, K. F., editors, *Shotcrete for Underground Support XI*, ECI Symposium Series, pages 1–18, June 2009.
- [341] SBT 1.1 Tunnel Gloggnitz: ARGE. Semmering Base Tunnel, construction lot SBT 1.1, tunnel Gloggnitz—Daily construction records. Project document (in german), Joint venture (ARGE): Implenia Österreich GmbH, HOCHTIEF Infrastructure GmbH, THYSSEN SCHACHTBAU GMBH, 2016.
- [342] SBT 1.1 Tunnel Gloggnitz: ARGE. Semmering Base Tunnel, construction lot SBT 1.1, tunnel Gloggnitz—Daily construction records. Project document (in german), Joint venture (ARGE): Implenia Österreich GmbH, HOCHTIEF Infrastructure GmbH, THYSSEN SCHACHTBAU GMBH, 2017.
- [343] SBT 1.1 Tunnel Gloggnitz: PGST. Semmering Base Tunnel, construction lot SBT 1.1, tunnel Gloggnitz—Tender documents: Geotechnical prognosis underground. Project document (in german), Austrian Federal Railways, 2014. Planungsgemeinschaft Semmering-Basistunnel neu Tunnelbau (PGST).
- [344] SBT 1.1 Tunnel Gloggnitz: site team. Semmering Base Tunnel, construction lot SBT 1.1, tunnel Gloggnitz—Presentation for the 13th meeting on the geotechnical conditions. Project document (in german), 2016.

BIBLIOGRAPHY 310 of 498

[345] SBT 1.1 Tunnel Gloggnitz: site team. Semmering Base Tunnel, construction lot SBT 1.1, tunnel Gloggnitz—Report on the site decisions on support. Project document (in german), 2016.

- [346] SBT 1.1 Tunnel Gloggnitz: site team. Semmering Base Tunnel, construction lot SBT 1.1, tunnel Gloggnitz—Report on the site decisions on support. Project document (in german), 2017.
- [347] Schädlich, B. and Schweiger, H. F. Shotcrete Model: Implementation, validation and application. Internal technical report, Graz University of Technology, Graz, Austria, October 2016.
- [348] Schädlich, B. and Schweiger, H. F. A new constitutive model for shotcrete. In Hicks, M. A., Brinkgreve, R. B. J., and Rohe, A., editors, Numerical Methods in Geotechnical Engineering Proceedings of the 8th European Conference on Numerical Methods in Geotechnical Engineering, NUMGE 2014, volume 1, pages 103–108, Delft, Netherlands, June 2014. Taylor & Francis Group, London, UK.
- [349] Schädlich, B., Schweiger, H. F., Marcher, T., and Saurer, E. Application of a novel constitutive shotcrete model to tunnelling. In *Rock Engineering and Rock Mechanics:* Structures in and on Rock Masses, pages 799–804. CRC Press, May 2014.
- [350] Schanz, T., Vermeer, P. A., and Bonnier, P. G. The hardening soil model: Formulation and verification. In *Proceedings of the 1st PLAXIS symposium: Beyond 2000 in Computational Geotechnics-10 Years of PLAXIS*, pages 1–16. Balkema: Rotterdam, 1999.
- [351] Scheiner, S. and Hellmich, C. Continuum Microviscoelasticity Model for Aging Basic Creep of Early-Age Concrete. *Journal of Engineering Mechanics*, 135(4):307–323, April 2009.
- [352] Scheydt, J. C. Influence of the reactive Components on Shotcrete Performance. *Tunnel*, (3):22–27, 2015.
- [353] Schlicke, D. Mindestbewehrung für zwangbeanspruchten Beton: Festlegung unter Berücksichtigung der erhärtungsbedingten Spannungsgeschichte und der Bauteilgeometrie. In Monographic Series TU Graz, Schriftenreihe des Instituts für Betonbau, volume 4. Verlag der Technischen Universität Graz, Graz, Austria, 2nd edition, 2016.
- [354] Schlicke, D. Personal communication, February 2018.
- [355] Schlicke, D. Personal communication, June 2020.
- [356] Schmid, S. M. and Handy, M. R. Controversies in Modern Geology. Evolution of Geological Theories in Sedimentology, Earth History and Tectonics., chapter 16. Towards a Genetic Classification of Fault Rocks: Geological Usage and Tectonophysical Implications, pages 339–361. Academic Press Limited, London, 1991.
- [357] Schön, J. H. Developments in Petroleum Science. In Physical Properties of Rocks-Fundamentals and Principles of Petrophysics, volume 65. Elsevier B.V., 2nd edition, December 2015.
- [358] Schubert, P. Beitrag zum rheologischen Verhalten von Spritzbeton. Felsbau, 6(3):150–153, 1988.

BIBLIOGRAPHY 311 of 498

[359] Schubert, P., Hölzl, H., Sellner, P., and Fasching, F. Geomechanical knowledge gained from the Paierdorf investigation tunnel in the section through the Lavanttal main fault zone. *Geomechanics and Tunnelling*, 3(2):163–173, April 2010.

- [360] Schubert, W. Erfahrungen bei der Durchörterung von Störzonen bei österreichischen Tunneln. In Proceedings of the "Nachdiplomkurs in angewandten Erdwissenschaften: Herausforderung Geologie im Untertagebau", pages 1–10, CSF Monte Veritá, Ascona, Switzerland, May 1996. ETH Zurich.
- [361] Schubert, W. Experience of tunnel construction in weak ground. Geomechanics and Tunnelling, 4(3):211–220, June 2011.
- [362] Schubert, W. and Riedmüller, G. Geotechnisches Gutachten zum Verbruch Galgenbergtunnel / Vortrieb Leoben Ost Sta. 1326 bis 1333,6. Technical report, The Austrian Federal Railways, Graz, Austria, April 1995. Unpublished.
- [363] Schubert, W. and Riedmüller, G. Geotechnische Nachlese eines Verbruches Erkenntnisse und Impulse. In Semprich, S., editor, *Proceedings of the 10th Christian Veder Colloquium: Innovation in der Geotechnik Entwicklungen der letzten Jahre*, number 13 in Mitteilungshefte, pages 59–68, Graz, Austria, 1995. Institute of Soil Mechanics and Foundation Engineering, Graz University of Technology.
- [364] Schubert, W. and Riedmüller, G. Tunnelling in Fault Zones State of the Art in Investigation and Construction. Felsbau, 18(2):7–15, 2000.
- [365] Schubert, W., Brandtner, M., Schweiger, H. F., Helmberger, A., Marcher, T., and Radončić, N. Proposed design strategy for tunnels. In Schubert, W. and Kluckner, A., editors, Proceedings of the ISRM Regional Symposium EUROCK 2015 & 64<sup>th</sup> Geomechanics Colloquium— Future Development of Rock Mechanics, pages 37–47, Salzburg, Austria, October 2015. Austrian Society for Geomechanics.
- [366] Schubert, W., Blümel, M., Brunnegger, S., Staudacher, R., and Sellner, P. J. Aspekte des Ausbaus. In Schubert, W. and Kluckner, A., editors, *Proceedings of the Workshop on Tunnelbau in Störungszonen—Eine Herausforderung*, pages 49–62, Graz, Austria, November 2016. Institute of Rock Mechanics and Tunnelling, Graz University of Technology.
- [367] Schubert, W., Blümel, M., Staudacher, R., and Brunnegger, S. Support aspects of tunnels in fault zones. *Geomechanics and Tunnelling*, 10(4):342–352, August 2017.
- [368] Schütz, R., Potts, D. M., and Zdravković, L. Advanced constitutive modelling of shotcrete: Model formulation and calibration. *Computers and Geotechnics*, 38(6):834–845, September 2011.
- [369] Schütz, R. Numerical Modelling of Shotcrete for Tunnelling. PhD thesis, Imperial College London, London, UK, February 2010.
- [370] Sercombe, J., Hellmich, C., Ulm, F.-J., and Mang, H. A. Modeling of early-age creep of shotcrete. I: Model and model parameters. *Journal of Engineering Mechanics*, 126(3): 284–291, 2000.
- [371] Sezaki, M., Kibe, T., Ichikawa, Y., and Kawamoto, T. An experimental study on the mechanical properties of shotcrete. *Journal of the Society of Materials Science*, 38(434): 1336–1340, 1989.

BIBLIOGRAPHY 312 of 498

[372] Sibson, R. H. Fault rocks and fault mechanisms. *Journal of the Geological Society*, 133(3): 191–213, March 1977.

- [373] Sibson, R. H. Structural permeability of fluid-driven fault-fracture meshes. *Journal of Structural Geology*, 18(8):1031–1042, August 1996.
- [374] Simo, J. C., Kennedy, J. G., and Govindjee, S. Non-smooth multisurface plasticity and viscoplasticity. Loading/unloading conditions and numerical algorithms. *International Journal for Numerical Methods in Engineering*, 26(10):2161–2185, October 1988.
- [375] Skempton, A. W. Residual strength of clays in landslides, folded strata and the laboratory. *Géotechnique*, 35(1):3–18, March 1985.
- [376] Sönmez, H., Gokceoglu, C., Tuncay, E., Medley, E. W., and Nefeslioglu, H. A. Relationships between Volumetric Block Proportions and Overall UCS of a Volcanic Bimrock. *Felsbau*, 22(5):27–34, 2004.
- [377] Sönmez, H., Tuncay, E., and Gokceoglu, C. Models to predict the uniaxial compressive strength and the modulus of elasticity for Ankara Agglomerate. *International Journal of Rock Mechanics and Mining Sciences*, 41(5):717–729, July 2004.
- [378] Sönmez, H., Gokceoglu, C., Medley, E. W., Tuncay, E., and Nefeslioglu, H. A. Estimating the uniaxial compressive strength of a volcanic bimrock. *International Journal of Rock Mechanics and Mining Sciences*, 43(4):554–561, June 2006.
- [379] Sönmez, H., Kasapoglu, K. E., Coskun, A., Tunusluoglu, C., Medley, E. W., and Zimmerman, R. W. A conceptual empirical approach for the overall strength of unwelded bimrocks. In Vrkljan, I., editor, Proceedings of the 2009 Regional Symposium of the International Society for Rock Mechanics (EUROCK 2009)—Rock Engineering in Difficult Ground Conditions Soft Rocks and Karst, pages 357–360, Dubrovnik, Croatia, October 2010. Taylor & Francis: London.
- [380] Stadlmann, T., Vanek, R., and Goricki, A. Semmering Base Tunnel, construction lot SBT 1.1, tunnel Gloggnitz—Tender documents: Rock mass types. Project document (in german), Austrian Federal Railways, 2014.
- [381] Staudacher, R. F. Anschlüsse für Arbeitsfugen bei Spritzbetonauskleidungen. Master's thesis, Graz University of Technology, Graz, Austria, November 2016.
- [382] Steindorfer, A. F. Short Term Prediction of Rock Mass Behaviour in Tunnelling by Advanced Analysis of Displacement Monitoring Data. PhD thesis, Graz University of Technology, Graz, Austria, November 1997.
- [383] Stini, J. Tunnelbaugeologie Die geologischen Grundlagen des Stollen- und Tunnelbaues. Springer Vienna, 1st edition, 1950.
- [384] Swanson, M. T. Late Paleozoic strike-slip faults and related vein arrays of Cape Elizabeth, Maine. *Journal of Structural Geology*, 28(3):456–473, March 2006.
- [385] Tazawa, E.-i., editor. Autogenous Shrinkage of Concrete: Proceedings of the International Workshop, organized by the JCI (Japan Concrete Institute), Hiroshima, Japan, June 1999. Taylor & Francis.
- [386] Terzaghi, K. Theoretical Soil Mechanics. John Wiley & Sons, Inc.: New York, 1943.

BIBLIOGRAPHY 313 of 498

[387] Thomas, A. Numerical modelling of sprayed concrete lined (SCL) tunnels. PhD thesis, University of Southampton, Southampton, United Kingdom, 2003.

- [388] Thomas, A. Sprayed Concrete Lined Tunnels—An introduction. Taylor & Francis, 2009.
- [389] Thomas, A. Sprayed Concrete Lined Tunnels—second edition. CRC Press, 2020.
- [390] Thomée, B. *Physikalisch nichtlineare Berechnung von Stahlfaserbetonkonstruktionen*. PhD thesis, Technical University Munich, Munich, Germany, 2005.
- [391] Thornton, C. Numerical simulations of deviatoric shear deformation of granular media. Géotechnique, 50(1):43–53, February 2000.
- [392] Thuro, K., Plinninger, R. J., Zäh, S., and Schütz, S. Scale effects in rock strength properties. Part 1: Unconfined compressive test and Brazilian test. In Särkkä and Eloranta, editors, Proceedings of the 2001 Regional Symposium of the International Society for Rock Mechanics (EUROCK 2001)—Rock Mechanics A Challenge for Society, pages 169–174. Swets & Zeitlinger Lisse, 2001.
- [393] Tigges, V. E. Die Hydratation von Hüttensanden und Möglichkeiten ihrer Beeinflussung zur Optimierung von Hochofenzementeigenschaften. PhD thesis, Clausthal University of Technology, Clausthal-Zellerfeld, Germany, 2009.
- [394] Tourenq, C. and Denis, A. La resistance a la traction des roches. Rapport de Recherches 4A, Laboratoire Central des Ponts et Chaussées, Paris, France, 1970.
- [395] Traina, L. A. Experimental stress-strain behaviour of a low strength concrete under multiaxial states of stress. Technical report AFWL-TR-82-92, Air Force Weapons Laboratory, Kirtland Air Force Base, New Mexico, USA, 1983.
- [396] Tsesarsky, M., Hazan, M., and Gal, E. Estimating the elastic moduli and isotropy of block in matrix (bim) rocks by computational homogenization. *Engineering Geology*, 200:58–65, January 2016.
- [397] Twiss, R. J. and Moores, E. M. Structural Geology. W. H. Freeman and Company, New York, USA, 2nd edition, 2007.
- [398] Tziallas, G. P., Tsiambaos, G., and Saroglou, H. Determination of Rock Strength and Deformability of Intact Rocks. *Electronic Journal of Geotechnical Engineering (EJGE)*, 14 (G):1–12, 2009.
- [399] Ulm, F.-J. Couplages thermochémomécaniques dans les bétons: Un premier bilan. Monograph LCPC OA31, Laboratoire Central des Ponts et Chaussées, Paris, France, 1998.
- [400] Ulm, F.-J. and Acker, P. Le point sur le fluage et la recouvrance des bétons. *Bulletin Liaison des Laboratoires des Ponts et Chaussées*, (XX):73–82, 1998. Special issue.
- [401] Ulm, F.-J. and Coussy, O. Modeling of Thermochemomechanical Couplings of Concrete at Early Ages. *Journal of Engineering Mechanics*, 121(7):785–794, 1995.
- [402] Ulm, F.-J. and Coussy, O. Strength Growth as Chemo-Plastic Hardening in Early Age Concrete. *Journal of Engineering Mechanics*, 122(12):1123–1132, 1996.

BIBLIOGRAPHY 314 of 498

[403] Ulusay, R., Türeli, K., and Ider, M. H. Prediction of engineering properties of a selected litharenite sandstone from its petrographic characteristics using correlation and multivariate statistical techniques. *Engineering Geology*, 38(1-2):135–157, December 1994.

- [404] U.S. Department of the Interior Bureau of Reclamation. *Engineering geology field manual*, volume I. U.S. Government Printing Office, 2nd edition, 1998.
- [405] U.S. Department of the Interior Bureau of Reclamation. Glossary of commonly used terms by the Bureau of Reclamation. Electronical, 2016. URL https://www.usbr.gov/library/glossary/index.html. Last access: 20.12.2016.
- [406] van der Pluijm, B. A. and Marshak, S. Earth structure: an introduction to structural geology and tectonics. W. W. Norton & Company, Inc.: New York, 2nd edition, 2004.
- [407] Vanek, R. and Stadlmann, T. Semmering Base Tunnel new—Legal railway approval procedure documents: Report on the construction geology. Project document (in german), Austrian Federal Railways, May 2010.
- [408] Vanek, R., Fasching, F., and Fasching, A. Ingenieurgeologische Charakterisierung von Störungszonen. In Schubert, W. and Kluckner, A., editors, *Proceedings of the Workshop on Tunnelbau in Störungszonen—Eine Herausforderung*, pages 1–11, Graz, Austria, November 2016. Institute of Rock Mechanics and Tunnelling, Graz University of Technology.
- [409] VBE. Semmering Base Tunnel, construction lot SBT 1.1, tunnel Gloggnitz—Concrete test report. Project document (in german), Verein für Baustoffprüfung und -entwicklung (VBE), 2016.
- [410] Vermeer, P. A. and de Borst, R. Non-associated plasticity for soils, concrete and rock. HERON, 29(3):1–64, 1984.
- [411] Vlachopoulos, N. and Diederichs, M. S. Improved Longitudinal Displacement Profiles for Convergence Confinement Analysis of Deep Tunnels. Rock Mechanics and Rock Engineering, 42(2):131–146, April 2009.
- [412] Volpe, R., Ahlgren, C., and Goodman, R. Selection of engineering properties for geologically variable foundations. In *Proceedings of the 17th International Congress on Large Dams*, *Vienna:Paris*, pages 1087–1101. International Commission on Large Dams, 1991.
- [413] von Rabcewicz, L. Die Ankerung im Tunnelbau ersetzt bisher gebräuchliche Einbaumethoden. Schweizerische Bauzeitung, 75(9):123–131, March 1957.
- [414] von Terzaghi, K. *Ingenieurgeologie*, chapter Tunnelgeologie, pages 365–407. Julius Springer: Vienna, 1st edition, 1929.
- [415] Wagner, L. Concept and realisation of a distributed fibre-optic sensing system for direct and continuous strain measurement in a shotcrete lining. Master's thesis, Graz University of Technology, Graz, Austria, September 2017.
- [416] Wagner, L., Kluckner, A., Monsberger, C. M., Wolf, P., Prall, K., Schubert, W., and Lienhart, W. Direct and Distributed Strain Measurements Inside a Shotcrete Lining: Concept and Realisation. *Rock Mechanics and Rock Engineering*, 53(2):641–652, August 2019.

BIBLIOGRAPHY 315 of 498

[417] Wen-jie, X., Zhong-qi, Y., and Rui-lin, H. Study on the mesostructure and mesomechanical characteristics of the soil—rock mixture using digital image processing based finite element method. *International Journal of Rock Mechanics and Mining Sciences*, 45(5):749–762, July 2008.

- [418] Wen-Jie, X., Qiang, X., and Rui-Lin, H. Study on the shear strength of soil—rock mixture by large scale direct shear test. *International Journal of Rock Mechanics and Mining Sciences*, 48(8):1235–1247, December 2011.
- [419] Wesche, K. Baustoffe für tragende Bauteile—Band 2: Beton, Mauerwerk. Bauverlag GmbH: Wiesbaden, Berlin, 3rd edition, 1993.
- [420] Wibberley, C. A. J., Yielding, G., and Toro, G. D. Recent advances in the understanding of fault zone internal structure: a review. *Geological Society, London, Special Publications*, 299(1):5–33, 2008.
- [421] Wittmann, F. Bestimmung physikalischer Eigenschaften des Zementsteins. In *Deutscher Ausschuss für Stahlbeton*, number 232. Wilhelm Ernst & Sohn, Berlin, 1974.
- [422] Wuilpart, M. Advanced Fiber Optics: Concepts and Technology, chapter Rayleigh scattering in optical fibers and applications to distributed measurements, pages 1–56. EPFL Press, Lausanne, Switzerland, 1st edition, 2011.
- [423] Wullschläger, D. Ein Verbundwerkstoffmodell für die Systemankerung im Tunnelbau. PhD thesis, Universität Karlsruhe, Karlsruhe, Germany, 1988.
- [424] Yin, J. Untersuchungen zum zeitabhängigen Tragverhalten von tiefliegenden Hohlräumen im Fels mit Spritzbetonausbau. PhD thesis, Technische Universität Clausthal, Clausthal-Zellerfeld, Germany, February 1996.
- [425] ZAMG. Zentralanstalt für Meteorologie und Geodynamik: Klimamonitoring. Electronical, 2021. URL https://www.zamg.ac.at/cms/de/klima/klima-aktuell/klimamonitoring/?view=fullscreen&param=t&period=period-ymd-2016-11-17&ref=3. Last access: 02.12.2021.
- [426] Zhang, H.-Y., Xu, W.-J., and Yu, Y.-Z. Triaxial tests of soil—rock mixtures with different rock block distributions. *Soils and Foundations*, 56(1):44–56, February 2016.
- [427] Zhao, X. G. and Cai, M. A mobilized dilation angle model for rocks. *International Journal of Rock Mechanics and Mining Sciences*, 47(3):368–384, April 2010.
- [428] Zi, G. and Bažant, Z. P. Continuous Relaxation Spectrum for Concrete Creep and its Incorporation into Microplane Model M4. *Journal of Engineering Mechanics*, 128(12): 1331–1336, December 2002.